공학박사 학위논문

Near real-time estimation and optimization of microalgal photobioreactor system for productivity improvement

미세조류 배양 광생물반응기 시스템의 생산성 향상을 위한 근 실시간 추정 및 최적화

2015년 8월

서울대학교 대학원
화학생물공학부
유 성 진

Near real-time estimation and optimization of microalgal photobioreactor system for productivity improvement

지도교수 이종민

이 논문을 공학박사 학위논문으로 제출함

2015년 7월

서울대학교 대학원

화학생물공학부

유 성 진

유 성 진의 박사 학위논문을 인준함

2015년 8월

위 원 장	김 화 용	(인)
부위원장	이 종 민	(인)
위 원	이 윤 우	(인)
위 원	문 성 용	(인)
위 원	이 창 준	(인)

Abstract

Near real-time estimation and optimization of microalgal photobioreactor system for productivity improvement

Sung Jin Yoo
School of Chemical and Biological Engineering
The Graduate School
Seoul National University

This thesis has presented the near real-time optimization procedures for productivity improvement of microalgal photobioreactor system under mixotrophic cultivation. Microalgae have been suggested as a promising feedstock for producing biofuel because of their potential for lipid production. However, the development of large-scale algal biodiesel production has been limited by the high production cost of algal biomass. Therefore it is necessary to improve the economic feasibility by reducing costs or increasing productivity. In order to have an economically sound algal bioprocess, this thesis tries to optimize the operating conditions by manipulating nutrient (carbon and nitrogen sources) flow rates and light intensity. For this purposes, it is need to develop a dynamic model that describes algal growth and lipid accumulation in order to support the development of algal bioprocesses, their scale up, optimization and control. However, there are some difficulties in applying model-based control strategies to

microalgal cultivation systems. Microalgae cultivation systems are network of complex biochemical reactions manipuated by enzyme kinetics. Modelling of these complex biological systems accurately is difficult task since metabolism inside the cells makes systems have uncertainties. In addition to model uncertainties arising from complex biosystem dynamics, on-line measurement of important variables, especially in lipid is limited and difficult to realize in practice, which makes optimal bioreactor operation a challenging task. To cope with such problems, this thesis focused on the modelling, estimation of lipid concentration, and optimization of photobioreactor systems.

At first, the model was developed based on the Droop model, and the optimal input design using D-optimality criterion was performed to compute the system input profile, to estimate parameters more accurately. From the experimental observations, the newly defined yield coefficient was suggested to represent the consumption of lipid and nitrogen within the cell, which reduces the number of parameters with more accurate prediction. Furthermore, the lipid consumption rate was introduced to reflect the experimental results that lipid consumption is related to carbon source concentration. The model was validated with experiments designed with different initial conditions of nutrients and input changes, and showed good agreement with experimental observations.

After that, estimation of lipid concentration from other measurable sources such as biomass or glucose sensor was studied. Extended Kalman Filter (EKF), Unscented Kalman Filter (UKF), and Particle Filter (PF) were compared in various cases for their applicability to photobioreactor systems. Furthermore, simulation studies to identify appropriate types of sensors for estimating lipid were also performed.

Finally, to maximize the biomass and lipid concentration, various optimization methods were investigated in microalgal photobioreactor system under mixotrophic conditions. Lipid concentration was estimated using UKF with other measurable sources and used as lipid data for performing model predictive control (MPC). In addition, maximized biomass and lipid trajectory obtained by open-loop optimization was used as a reference trajectory for traking by MPC. Simulation studies with experimental validation were performed in all cases and significant improvement in productivities of biomass and lipid was obtained when MPC applied. However, it was observed that lag phase occurs while manipulating feed flow rate, which considered to come from large amount of inputs introduced suddenly. This is important phenomena can make model-plant mismatches and needs to be researched more for the optimization of microalgal photobioreactor in reality.

Keywords: Microalgae, Droop model, optimal input design, parameter estimation, sensor, Model predictive control, lag phase
Student Number: 2010-31013

Contents

List of Figures

List of Tables

Chapter 1

Introduction

Microalgae are photosynthetic microorganisms, which can produce large amounts of lipids that can be used directly as high value bioactives, or be used to synthesize biodiesel. As worldwide interest in alternative fuels has increased, the attention to microalgae as a feedstock for biodiesel is growing recently. The lipid contents in microalgae range from 15 wt% to 77 wt%, depending on the species or culture conditions [1]. Although the lipid production rate in microalgae is strain dependent, it has several advantages as a feedstock for biodiesel, including high growth rate and the ability to produce large amounts of lipid [2, 3, 4]. However, biodiesel from microalgae is not economically competitive compared to biodiesel from conventional plant sources or petrodiesel [1]. For economic competitiveness, it is necessary to improve the cell's growth rate or productivity of lipid by operating the bioreactor at optimal conditions. The process optimization and metabolic engineering are two complementary approches to enhance productivity of bioreactors and a dynamic model is an essential element in both approaches [5]. A mathematical model that describes algal growth and lipid accumulation is useful for predicting the productivities of microalgae, optimizing the cultivation conditions, and scaling up for industrial production.

Microalgae can be grown under autotrophic, heterotrophic, or mixotrophic growth conditions. Compared to autotrophic cultivation, heterotrophic and mixotrophic cultivations allow some microalgae to accumulate much higher lipid content, as well as to provide high biomass productivity [2, 6, 7]. In the case of $Chlorella\ protothecoides$, heterotrophic cultivation with glucose as an organic carbon source results in four times higher lipid contents than autotrophic cells, and the color of heterotrophic cells (yellow) differs from autotrophic cells (green) [2]. Under autotrophic growth conditions, growth is limited by light availability; the growth rate is reduced during night or in dark areas. However, under mixotrophic conditions, microalgae can use organic carbon sources to support their growth even in the night or dark areas. It was reported that only few microalgae can be cultivated mixotrophically, and among them are freshwater flagellate $Haematococcus\ pluvialis$, $C.\ protothecoides$, and $Ochromonas\ minima$ [8].

Lipid productivity of microalgae is also influenced by nitrogen. The nitrogen deficiency reduces cells growth rate, but the content of the lipid increases [9, 10]. Therefore, there is a trade-off relationship between growth rate and lipid productivity, and how to increase lipid content while maintaining cells growth properly by manipulating nitrogen concentrations is an important optimization problem.

In this thesis, microalgal photobioreactor model based on mixotrophic cultivation was proposed for the purpose of optimizing biomass and lipid productivities. As the dynamics of lipid are relatively fast, it would have a significant impact on the improvement of lipid productivity if real-time information on lipid concentration can be known [11]. However, researches about improvement of lipid productivity by

real-time monitoring and control with experimental validation is limited because measurement of lipid in microalgae is very difficult and time consuming task. When some inportant variables are not available from measurement, soft sensors can give an on-line estimation of the unmeasurable variables or model parameters from more easily accessible measurements and estimation algorithms [12, 13, 14]. The estimation algorithms (extended Kalman filter (EKF), unscented Kalman filter (UKF), particle filter (PF)) used in this study are already existent and actively researched algorithms but very few studies about application of them to lipid estimation was performed. Above all, lipid estimation together with experimental validation was performend in this study. For the estimation of lipid concentrations, on-line measurement of cell mass and off-line data of glucose concentration were used as measurement data with photobioreactor model and estimation algorithms.

Based on the microlagal photobioreactor model and lipid information estimated from non-linear estimator, optimization of photobioreactor was performed for productivity improvement of biomass and lipid in chap. 5. Various optimizaiton methods were compared; at first, microalgae were cultivated based on author's experience. Generally, it was known that nitrogen dificiency condition reduces the cell growth rate, but increases the amount of lipid [9, 10]. Reflecting this point, nitrogen feed was supplied from the beginning to the middle of the cultivation process while carbon source feed was supplied whole the cultivation process. The intention of this is to stimulates growth of microalgae initially and then changed it to the lipid. Secondly, open-loop optimization was performed. Using the photobioreactor model and parameters, the optimal input trajectories of the two

nutrient feeds and light intensity were calculated for the maximizing the biomass and lipid concentration. Finally, for the purpose of control of the photobioreactor, model predictive control is implemented. While microalgae were cultivated, there are many chances of occuring unknown metabolic reactions or phenomena which makes model mismatches to the real plant. In such case, model predictive control can be used to track the reference trajectory. Model predictive control uses model to predict future behaviour of the system and optimize the input actions in order to give optimal action to reach a desired target. In this study, maximized biomass and lipid trajectory obtained by applying optimal inputs calcultated from open-loop optimization method were used as reference trajectory.

Chapter 2

Experiment and data anlysis

2.1 Microalgae and media composition

Figure 1: $Chlorella\ protothecoides$ from UTEX

$Chlorella\ protothecoides$, UTEX B25 (UTEX Culture Collection of Algae, Texas) in Fig. 1, were cultivated under mixotrophic conditions. This strain was known to have large amount of lipid depending on culture conditions , and in this study it was cultivated under mixotrophic condition which use both heterotrophic and autotrophic means to support growth and maintenance. $C.\ protothecoides$

maintained on agar plates with proteose medium were subcultured in a flask with 150 ml culture media as in Fig. 2, and incubated at $25°\mathrm{C}$ and 200 rpm for 96 hrs. The composition of the culture media was as follows : KH_2PO_4 (2.8 g/L), K_2HPO_4 (1.2 g/L), $MgSO_4{\cdot}7H_2O$ (1.2 g/L), $FeSO_4{\cdot}7H_2O$ (48 mg/L), H_3BO_3 (11.6 mg/L), $CaCl_2{\cdot}2H_2O$ (10 mg/L), $MnCl_2{\cdot}4H_2O$ (7.2 g/L), $ZnSO_4{\cdot}7H_2O$ (0.88 mg/L), $CuSO_4$ $\cdot 5H_2O$ (0.32 mg/L), MoO_3 (72 μg/L), thiamine hydrochloride (40 μg/L), glucose (40 g/L), and glycine (0.5 g/L). All reagents were obtained from Sigma-Aldrich Co. and culture media were autoclaved at $121°\mathrm{C}$ for 15 mins.

Figure 2: Subculturing of $prototheco ides$ in a flask

2.2 Photobioreactor system and conditions

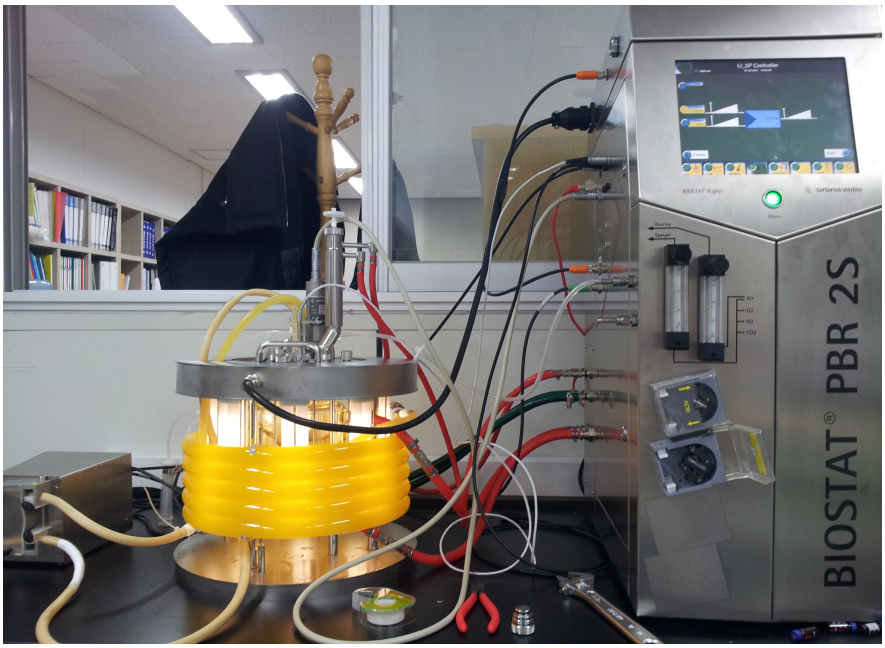

Figure 3: Photobioreactor system (Sartorious BIOSTAT PBR 2S)

C. protothecoides were cultivated in a photobioreactor system (Sartorious BIOSTAT PBR 2S, working volume 3L) in Fig. 3 with microalgae previously cultured in a flask as inoculum. The start-up medium had the same composition as the culture media, except for the glucose and glycine concentrations.

During operation of the photobioreactor, two feed flow rates and the light intensity were manipulated at a predefined time calculated from exprimental design. The feed flow rate 1, f_1^i, is the nitrogen source that contains only glycine. The feed flow rate 2, f_2^i, is for the carbon source supply that contains the same minerals with culture media, except glucose. The photobioreactor was aerated at a rate of

50 mL/min, which contains 10 % CO_2 by volume, and cultivated at $25°C$ for 12 days. During the cultivation, 40 mL of microalgae was sampled every 12 h for data analysis and represented in Fig. 4.

Figure 4: Sampled microalgae

2.3 Method for data analysis

2.3.1 Biomass measurement

Biomass concentration was measured using two different ways. First method use the dry weight calculation of microalgae. 15 mL of sampled microalgae was centrifuged at 4000 rpm for 20 mins. Centrifugation sediments were washed twice with distilled water and re-centrifuged. The final precipitate were dried at $80°C$ oven for 24 hrs and weighed. Biomass concentration was also measured on-line using a turbidity sensor (FUNDALUX II, Sartorius) which delivered an OD measurement at a high sampling rate (5 s). Turbidity data was calibrated with the dry weight data previously obtained from microalgae samples.

2.3.2 Glucose measurement

The clear supernatant from centrifugation of sampled micralgae was filtered using a 0.22 μm syringe filter to remove any residuals in

the liquid. After that glucose concentrations in the filtered supernatant were measured using HPLC (High Pressure Liquid Chromatography, Agilent 1260 Infinity). For the measure of glucose concentration, Zorbax carbohydrate column (4.6mm ID, length 150 mm) at $30^{\circ}\mathrm{C}$ and a refractive index detector (RID) at $35^{\circ}\mathrm{C}$ were used. Acetonitrile and distilled water were mixed at a ratio of 75 to 25 and used as an eluent with a flowrate of 1.4 mL/min as mentioned in the user manual of Agilent zorbax carbohydrate analysis column.

2.3.3 Glycine measurement

The glycine concentration was also measured using HPLC with Zorbax Eclipse AAA column (4.6 mm ID, lenth 150 mm) and a variable wavelength detector (VWD). For the determination of glycine, 40 mM of Na_2HPO_4 solvent and a mixture of acetonitrile, methanol, and distilled water at a ratio of 45:45:10 were used as eluents. For the fluorescence detection of glycine, the automated OPA (Ortho Phthalaldehyde) derivatization method was applied[15].

2.3.4 Lipid measurement

The total lipid concentration in the cells was determined using fluorespectrometer [16]. For the detection of fluorescence, microalgae samples were stained with nile red solution. Nile red stains intracellular lipid droplets red and intensely fluoresce in a lipid rich environment. In this method, fluorescence intensity has a linear relationship with the lipid concentration. 0.15 mL of 10 μg/L nile red solution in ethanol and 2.7 mL of 30% (v/v) ethanol solution in water were added to 0.15 mL of each sample of microalgae. Samples were

incubated at $40^{\circ}\mathrm{C}$ for 10 mins, and analyzed using fluorespectrometer. Excitation and emission wavelengths were selected as 530 nm and 604 nm, respectively. The fluoresence intensity was calibrated using microalgae samples, whose lipid concentration had been previously determined gravimetrically. For calibration, 1 L of final microalgae sample was washed twice with distilled water and recentrifuged. The final precipitate were lyophilized using freeze dryer (Bondiro, Korea) and then ground the lyophilized samples using a mortar to obtain fine powder. Finally, lipid in microalgae powder was extracted using hexane and isopropanol as solvents and weighed [17, 18].

Figure 5: Fine powder of microalgae

Chapter 3

Modelling of photobioreactor system

3.1 Introduction

In this chapter, microalgal photobioreactor systems under mixotrophic conditions were investiated, for the purpose of developing a mathematical model that predicts biomass and lipid production. Compared to autotrophic cultivation, heterotrophic and mixotrophic cultivations allow some microalgae to accumulate much higher lipid content, as well as to provide high biomass productivity [2, 6, 7]. In the case of $Chlorella\ protothecoides$, heterotrophic cultivation with glucose as an organic carbon source results in four times higher lipid contents than autotrophic cells, and the color of heterotrophic cells (yellow) differs from autotrophic cells (green) [2]. Under autotrophic growth conditions, growth is limited by light availability; the growth rate is reduced during night or in dark areas. However, under mixotrophic conditions, microalgae can use organic carbon sources to support their growth even in the night or dark areas. It was reported that only few microalgae can be cultivated mixotrophically, and among them are freshwater flagellate $Haematococcus\ pluvialis$, $C.\ protothecoides$, and $Ochromonas\ minima$ [8].

Lipid productivity of microalgae is also influenced by nitrogen.

The nitrogen deficiency reduces cells growth rate, but the content of the lipid increases [9, 10]. Therefore, identifying a trade-off relationship between growth rate and lipid productivity is a key issue for optimizaing biodiesel productivity.

In order to explain cell growth in bioreactor systems, a large number of models have been proposed in the literature. Among them, the Monod and Droop models are most widely used in control applications, since they are simple enough to apply model-based control strategies. For algal systems, the Droop model explains cell growth as a two-step phenomenon; the uptake of nutrients first occurs in the cell, and then intracellular nutrient is used to support cell growth [19]. Recently, models including lipid fraction have been presented as the interest has focused on the lipid production in the microalgae. A modified model based on the Droop model is presented, to predict the neutral lipid fraction under nitrogen stress [20, 10]. A lipid production model considering the simultaneous effect of carbon and nitrogen on the growth rate is also reported [21, 22].

In this section, a mathematical model that predicts the cell growth rate and lipid productivity under mixotrophic conditions varying nutrient conditions (glycine and glucose) and light intensity with $C.\ prothothecoides$ as a strain was developed. The experiments were performed based on the optimal experimental design and model parameters were estimated. From the experimental results, a newly defined concept of time-varying yield coefficient was applied and obtained better prediction performance with less number of parameters. The lipid consumption rate is also introduced to the model. Finally, the model was validated with the experiments which were designed with different initial and input conditions.

3.2 Classic growth models

3.2.1 Monod model

The Monod model is one of the classic models used for modelling growth rate in a bioreactor. It introduces the concept of the limiting nutrient. If there is a causal relationship between nutrient exhaustion and end of growth, then the nutrient is said to be limiting [23]. An important characteristic of the Monod behaviour is that there is an upper limit to growth rate when the nutrient is in great excess and there is no growth when the nutrient concentration is zero. Using the Monod model, the biomass growth rate, μ, is given as follows [24]:

$$\mu = \mu_m \left(\frac{S}{K_s + S} \right) \tag{3.1}$$

where μ_m is the maximum growth rate and K_s is the nutrient concentration that supports half the maximum growth rate. Note that using Monod model; the growth rate is dependent on nutrient concentration in the media and not the concentration inside the cell.

The Haldane model is similar to the Monod model but with the addition of nutrient inhibition. Therefore, unlike Monod behaviour where there is a maximum growth rate at excess nutrient concentration, the growth rate decreases after a certain nutrient concentration. This implies that there is an optimal nutrient concentration at which the maximum growth occurs. Based on the Haldane model, it can be concluded that running the bioreactor in excess nutrient does not achieve the best performance with respect to biomass growth. Using the Haldane kinetics the biomass growth rate, μ, is given as follows

[25]:

$$\mu = \mu_m \left(\frac{S}{K_s + S + \frac{S^2}{K_I}} \right) \tag{3.2}$$

where K_I is the inhibition constant. Even in the Haldane kinetics, the growth rate is dependent on extracellular nutrient concentration.

3.2.2 Cell quota model

The Monod and Haldane models have been widely used to model bacterial bioreactors; however, there is a clear difference in the dynamics of bacterial and algal systems. Microalgae exhibit a phenomenon called "luxury consumption" that is the initial uptake rates of a nutrient are far in excess of the organism's growth rate [19]. This is evident for nutrients such as phosphorus and nitrogen. In order to model this behaviour, the intracellular nutrient quota (q) is introduced as an intermediate state variable, in order to distinguish between nutrient uptake rate, ρ, and growth rate.

Droop model is the first proposed quota model and it is different from Monod model because it takes into account the notion of an internal nutrient pool. The growth and nutrient uptake rates using the Droop model are given below :

$$\mu = \mu_m \left(1 - \frac{k_q}{q} \right) \tag{3.3}$$

$$\rho = \rho_m \frac{S}{S + K_s} \tag{3.4}$$

where μ_m is the maximum growth rate based on intracellular nutrient quota (q) and not the nutrient concentration in the media (S). ρ_m is the

maximum uptake rate, K_s is the nutrient concentration that supports half the maximum uptake rate, and k_q is subsistence quota.

Another quota model was proposed by Caperon (1972). The Caperon model introduces concept of minimum quota required for growth and minimum extracellular nutrient concentration for nutrient uptake. The growth and nutrient uptake rates using the Caperon model are given below [26]:

$$\mu = \mu_m \left(\frac{q - q_0}{K_q + (q - q_0)} \right) \tag{3.5}$$

$$\rho = \rho_m \frac{S - S_0}{K_s + (S - S_0)} \tag{3.6}$$

where q_0 is the minimum nutrient quota at zero growth rate and K_q is the half saturation constant of nutrient quota for growth. S_0 is the nutrient concentration at which uptake rate is zero and K_s is the half saturation constant of extracellular nutrient concentration for nutrient uptake. The behaviour of cell-quota models is investigated in detail by Tett (1988).

3.3 Development of photobioreactor model

The photobioreactor system used in this study manipulates nitrogen source feed (glycine), carbon source feed (glucose), and light intensity as inputs and analyzes the biomass (X), glycine (S_1), glucose (S_2), and lipid concentrations (L) in the media as outputs. To represent this system the model was constructed having 13 parameters and 6 system states variables which are as follows :
1) x : functionally active biomass concentration (g/L)

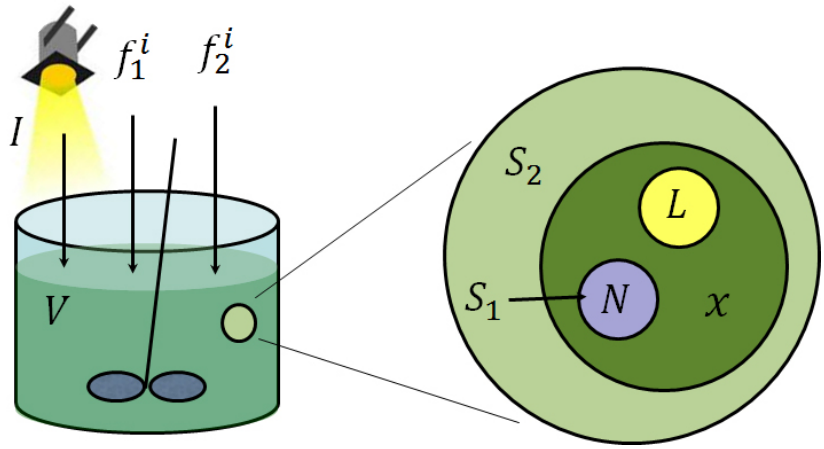

Figure 6: The description of photobioreactor system (semi-batch)

2) S_1 : nitrogen source concentration (glycine) in culture media (g/L)

3) S_2 : carbon source concentration (glucose) in culture media (g/L)

4) N : intracellular nitrogen concentration (g/L)

5) L : the amount of lipid stored in cells (g/L)

6) V : total reaction volume (L)

To predict the input-output relationship over the time course, a dynamic model firstly developed based on the Droop and Haldane model. To represent the photobioreactor system, the growth rate (μ) of functionally active biomass (x) which represents the carbon skeletons that are variously used to form other organic compounds was assumed to be affected by carbon, nitrogen, and light. While extracellular carbon source (glucose, S_2) directly affects the growth of active biomass as Michaelis-Menten relationship, this same assumption is not valid for nitrogen for algal systems[27]. The growth rate depends on the intracellular nitrogen quota $(q = N/X)$ as in the Droop model. To include the light effect, the model was developed taking

into account photoinhibition as in Eq. (3.7) [28].

$$\mu = \mu_m \left(1 - \frac{q_0}{q}\right) \left(\frac{S_2}{K_{S_2} + S_2}\right) \left(\frac{I}{K_I + I + \frac{I^2}{K_{Ii}}}\right) \tag{3.7}$$

where μ_m is the maximum growth rate, q_0 is the minimum nitrogen quota for growth, K_{S_2} is the half saturation constant of carbon source for growth, I is the light intensity, K_I is the half saturation constant of light for growth, and K_{Ii} is the light inhibition constant.

The uptake rate of the nitrogen source into the cells (ρ)is the same as in Droop model with an additional term to prevent unrealistic quota increase in the dark, and can be expressed as follows [29] :

$$\rho = \rho_m \left(\frac{S_1}{S_1 + K_{S_1}}\right) \left(\frac{q_m - q}{q_m - q_0}\right) \tag{3.8}$$

where S_1 is the extracellular glycine concentration with K_{S_1} the half saturation constant of glycine for uptake and q_m is the maximum quota of nitrogen above which the uptake rate stops.

The lipid production of $protothecoides$ increases under heterotrophic cultivation with glucose as a carbon source. Hence, the lipid production rate (π) is assumed to be a function of the carbon source concentration in culture media. It is known that lipid production is a light-independent reaction that light term is not considered in the lipid production rate [30]. Since the lipid production increases in nitrogen starvation conditions, the lipid production rate was assumed to decrease as more nitrogen exists in the cells. For the considering of saturation of lipid, the lipid production rate was assumed to decrease

as cells become saturated with lipid and represented as follows.

$$\pi = \pi_m \left(\frac{S_2}{K_\pi + S_2} \right) \left(1 - \frac{N}{X} \right) \left(1 - \frac{L}{X} \right) \tag{3.9}$$

where π_m is the maximum lipid production rate and K_π is the half saturation constant of glucose for lipid production. The total biomass concentration, X, is defined as

$$X = x + N + L \tag{3.10}$$

The dynamics of the photobioreactor can be expressed from mass balance considerations as follows :

$$\begin{aligned}
\frac{dx}{dt} &= \mu x - xD \\
\frac{dS_1}{dt} &= -\rho x + S_1^i \frac{f_1^i}{V} - S_1 D \\
\frac{dS_2}{dt} &= -\frac{1}{Y_{xs}} \mu x - \frac{1}{Y_{ls}} \pi x + S_2^i \frac{f_2^i}{V} - S_2 D \\
\frac{dN}{dt} &= \rho x - \frac{1}{Y_{xq}} \mu x - ND \\
\frac{dL}{dt} &= \pi x - LD \\
\frac{dV}{dt} &= VD - f_0
\end{aligned} \tag{3.11}$$

where D is the dilution rate (ratio of the influent flow rate over the volume) given by $D = (f_1^i + f_2^i)/V$, with f_1^i and f_2^i being the volumetric flow rate of glycine feed and glucose feed, respectively. S_1^i and S_2^i are the feed concentrations of glycine and glucose, respectively. f_0 is the outlet flow rate, and in this study, sampling was considered as

the single source of outlet flow.

3.4 Optimal experimental design

Optimal input design is a way to find a good estimate of parameters of the model by designing optimal trajectories of the inputs for the generation of experimental data. In this study, the optimal input signal was calculated using the D-optimality criterion [21, 31]. In parametric models the output sensitivity with respect to a parameter P is $\partial y/\partial P$, which determines how accurately parameters can be estimated from the input/output data. If the sensitivity of y with respect to parameter P is small, then the input sequence $u(t)$ is not designed enough to excite the parametric sensitivities sufficiently [32].

In this study, the four measured variables are the total biomass, glycine, glucose, and lipid concentrations as $y = [x{+}N{+}L, S_1, S_2, L]$. The photobioreactor model can be expressed using a state-space form as :

$$\begin{aligned} \dot{z} &= f(z, u, P) \\ y &= h(z, P) \end{aligned} \tag{3.12}$$

where z is the vector of state variables. Differentiation of f with respect to P using the chain rule yields [33]:

$$\frac{d}{dt}\left(\frac{\partial z}{\partial P}\right) = \frac{\partial f}{\partial z}\frac{\partial z}{\partial P} + \frac{\partial f}{\partial P} \tag{3.13}$$

The $\partial z/\partial P$ can be computed by integrating the sensitivity equations in Eq. (3.13). Then, $\partial y/\partial P$ can also be computed by differentiating

with respect to P using the chain rule as in Eq. (3.14).

$$\frac{\partial y}{\partial P} = \frac{\partial h}{\partial P} + \frac{\partial h}{\partial z}\frac{\partial z}{\partial P} \tag{3.14}$$

By computing $\partial y/\partial P$, the output sensitivity matrix (Z) can be expressed as in Eq. (3.15) which represents the effects of parameter values on the system outputs. The sampling time and total calculation time were chosen as 1 h and 12 days, respectively. Then, Z becomes a 1152×13 matrix.

$$Z = \begin{bmatrix} \left(\frac{\partial y_1}{\partial P_1}\right)\Big|_{t_1} & \cdots & \left(\frac{\partial y_1}{\partial P_{13}}\right)\Big|_{t_1} \\ & \vdots & \\ \left(\frac{\partial y_4}{\partial P_1}\right)\Big|_{t_1} & \cdots & \left(\frac{\partial y_4}{\partial P_{13}}\right)\Big|_{t_1} \\ & \vdots & \\ & \vdots & \\ \left(\frac{\partial y_1}{\partial P_1}\right)\Big|_{t_f} & \cdots & \left(\frac{\partial y_1}{\partial P_{13}}\right)\Big|_{t_f} \\ & \vdots & \\ \left(\frac{\partial y_4}{\partial P_1}\right)\Big|_{t_f} & \cdots & \left(\frac{\partial y_4}{\partial P_{13}}\right)\Big|_{t_f} \end{bmatrix} \tag{3.15}$$

The optimal input (u^*) can then be calculated by solving the optimization problem in Eq. (3.16), which maximizes the determinant of ($Z^T Z$). Among various statistical criteria, the D-optimal criterion seeks to minimize $|(X^T X)^{-1}|$, or maximize the determinant of the information matrix $X^T X$ of the design [31]. Because the input switch frequency was chosen as 12 h within 12 days of total calculation time, the number of optimization variables $(u_1, \ldots, u_f)$ was 54 and the optimization problem was solved using the genetic algorithm and pat-

tern search tool available in Matlab.

$$u^* = arg \max_{u \in U} \left| Z^T Z \right| \tag{3.16}$$

The designed optimal input signals obtained by solving the optimization problem are shown in Fig. 7. These input signals are implemented while performing experiments for the parameter estimation.

3.5 Parameter estimation

The parameters of the model were estimated by the weighted least square estimation method. The weighted sum of squared errors (WSSE) between measured data and model prediction was defined as the objective function and minimized.

$$WSSE(P) = \sum_{i=1}^{n} \sum_{j=1}^{m} (y_{ij} - \hat{y}_{ij})^T W_{ij} (y_{ij} - \hat{y}_{ij}) \tag{3.17}$$

where n is the number of experimental data points, m is the number of measured variables (four in this study), y_{ij} is the measured value of variable j at time i, and $\hat{y}_{ij}$ is the calculated value of variable j at time i from the model. The weighting factor, W_{ij}, was defined to assign more weights to measured variables with less variances and to balance the scales among measured variables as in Eq. (3.18).

$$W_{ij} = \frac{1}{\sigma_{ij} \lambda_j} \tag{3.18}$$

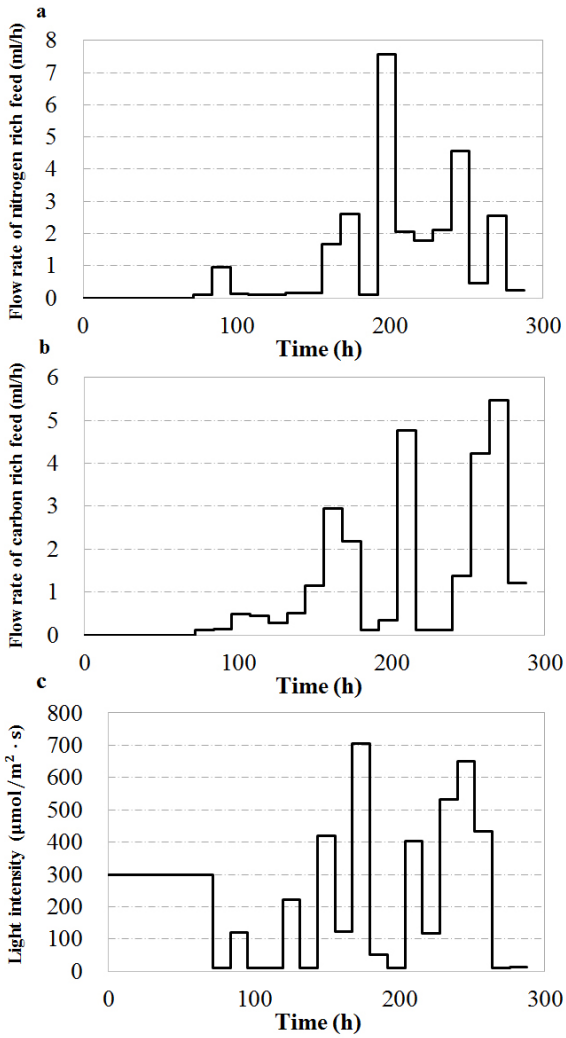

Figure 7: Designed optimal input signals for parameter estimation ((a) Flowrate of nitrogen rich feed; (b) Flowrate of carbon rich feed; (c) Light intensity)

where σ_{ij} is the standard deviation of the measurement variables and λ_j is a scaling factor for normalizing the measurement variables as in

Eq. (3.19).

$$\lambda_j = \frac{\sum_{i=1}^{n} |y_{ij} - \bar{y}_{ij}|}{\sum_{i=1}^{n} |y_{ij_r} - \bar{y}_{ij_r}|} \tag{3.19}$$

where y_{ij_r} is the measured variable used as a reference variable and $\bar{y}_{ij}$ is the mean value of the measurement variables. The standard deviation in Eq. (3.18) is calculated after normalizing the measured data. The optimization problem to minimize WSSE was solved using the pattern search tool in Matlab.

3.6 Results and Discussion

3.6.1 Simulation and experimental results

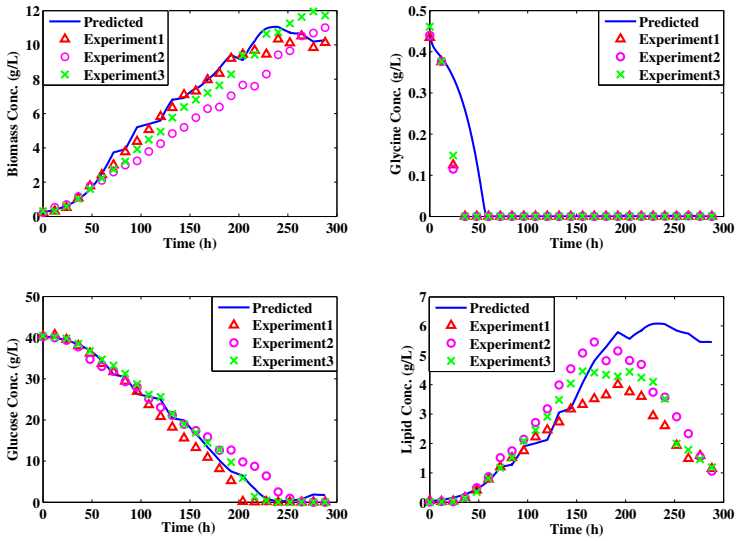

Figure 8: Comparison of experimental resuts and simulation results

$C. prototheco ides$ were cultivated in mixotrophic conditions with

the inputs shown in Fig. 7 to determine parameter values of the suggested photobioreactor model. The experiments were repeated three times with the same conditions : same initial culture conditions and same inputs to confirm the repeatability of experiments. The model simulation results and all experimental results are shown in Fig. 8. Although there are some discrepancies among the experimental results, it was observed that the experimental data points have similar trends in all three cases. In particular, the lipid concentration was decreased after 200 h in all cases.

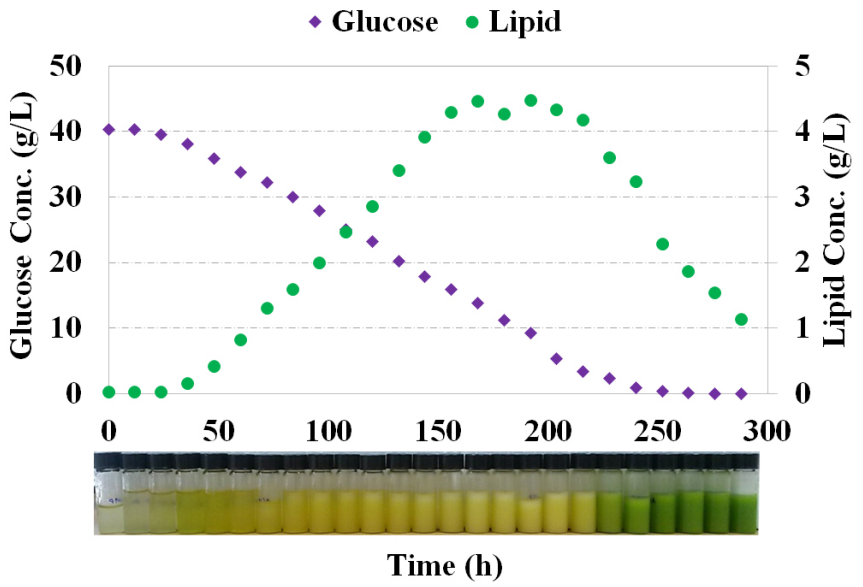

Figure 9: Relationship between color changes of microalgae and concentrations of lipid and glucose

Whereas the model predictions show good agreement with the concentrations of biomass, glycine, and glucose, the phenomenon of lipid depletion after 200 h is not explained. This is because the model

does not include any term representing lipid reductions. Fig. 9 shows the color changes of the algal samples together with the concentrations of glucose and lipid at different sample times. At the beginning of cultivation, the color of microalgae was green. As the lipid concentration increases, the color of microalgae turned yellow and lasted for some time. After that, as lipid concentration was decreased, the color turned green again. This observation coincides with the result reported in Miao and Wu (2006) that lipid rich $prothothecoides$ cultivated heterotrophically have yellow color. Moreover, in this study, the color of microalgae already turned to yellow changed to green again as the lipid decreased, which suggest that the lipid dynamic is relatively fast and is related to the color of microalgae. There are two possible reasons of lipid reduction after 200 h. The first is that large amount of nitrogen feed introduced after 200 h as in Fig. 7 makes cells accelerate the growth while reducing lipid. The second is related to the glucose concentration. The beginning point of lipid reduction is related to the point where the glucose is exhausted. This observation suggested that extracellular glucose was used as a nutrient for lipid as well as carbohydrate production in glucose rich conditions. However, in nutrient deficiency conditions, it was assumed that microalgae use accumulated lipid as a source for carbohydrate production.

3.6.2 Modification of the photobioreactor model

The microalgal photobioreactor model in Eqs. (3.7)-(3.11) were modified reflecting the experimental results related to the lipid reduction. The consumption of a substance can be related to the growth or production rate by introducing a yield coefficient. Consider a sim-

ple system with one nutrient and one product where the nutrient consumption is proportional to the production rate of the product. In such a system, a yield coefficient can be used as a constant to explain the consumption of nutrient. However, the total biomass is the sum of the active biomass, lipid, and nitrogen. It is more complicated to address the consumption of each substance inside the cell. To explain the consumption of nitrogen and lipid inside the cell, the yield coefficients of nitrogen to biomass, Y_{xq}, and lipid to biomass, Y_{xl}, can be multiplied by the growth rate. However, experimental results show that the assumption of constant yield coefficients may not be appropriate for this system. The yield coefficient, Y_{xl}, for the lipid is generally defined as

$$Y_{xl} = \frac{\Delta x}{\Delta L} \tag{3.20}$$

Then, the lipid consumption term can be expressed in mass balance equation as $-\frac{1}{Y_{xl}}\mu x$ with Y_{xl} as a constant. Instead of employing constants for yield coefficients over the entire range of operations, this study approximates the yields coefficients for lipid and nitrogen as

$$\begin{aligned} Y_{xl} &= \frac{\Delta x}{\Delta L} \approx \frac{x}{L} \\ Y_{xq} &= \frac{\Delta x}{\Delta N} \approx \frac{x}{N} \end{aligned} \tag{3.21}$$

This is not an exact expression of the definition of yield coefficients. However, it is very reasonable compared to just expressing them as constants because they reflect the time-varying value of the product within the cell. In particular, the real value of yield coefficient has a large difference between before and after lipid reduction, and cannot be expressed as just a constant. Furthermore, this can express the

consumption of each element more simply without additional parameters. Using Eq. (3.21), the nitrogen and lipid consumption terms in the mass balance equation can be expressed as $-\mu N$ and $-\mu L$ instead of $-\frac{1}{Y_{xq}}\mu x$ and $-\frac{1}{Y_{xl}}\mu x$, respectively. However, the application of this approach has a limitation in the range within intracellular phenomena. The reason that approximation of yield coefficient within cells is possible is that initial concentration of intracellular products is close to zero, which makes intracellular concentrations reflect the definition of yield coefficient at initial time. On the other hand, this approach cannot be applied to extracellular phenomena like glucose consumption for biomass production because initial concentration of glucose and biomass can't reflect the definition of yield coefficient.

The lipid consumption rate was introduced to explain lipid consumption in microalgae more accurately reflecting the experimental results. From Fig. 8, it was assumed that the lipid consumption rate is inversely proportional to the glucose concentration as in Eq. (3.22).

$$\nu = \nu_m \left(\frac{K_\nu}{S_2 + K_\nu} \right) \left(1 - \frac{l_0}{l} \right) \tag{3.22}$$

where ν_m is the maximum lipid consumption rate, K_ν is the half saturation constant of carbon source for lipid consumption, and l_0 is the minimum lipid quota for supporting growth.

The growth rate was modified by the rationale that the accumulated lipid was used in carbohydrate production and quota model ($l = L/X$) as in the nitrogen quota was assumed. The photoinhibition usually takes place in different light intensity according to microalgal species and cultivation conditions such as temperature and shape of bioreactor [34, 35]. The types of cultivation like au-

totrophic or mixotrophic also affect the photoinhibition and it was known that mixotrophic cultivation can protect photoinhibition by use carbon source as energy source rather than light [36, 37]. In this thesis, the microalgae was cultivated mixotrophically with dense cell concentration and fast circulation speed, which makes cells can protect from photoinhibition by mutual shading. Above all, model tests with and without photoinhibition term show almost no differences as in Fig. 10. Therefore, photoinhibition effect was ignored and modified growth rate was represented in Eq. (3.23).

$$\mu = \mu_m \left(1 - \frac{q_0}{q}\right)\left(1 - \frac{l_0}{l}\right)\left(\frac{S_2}{K_{S_2} + S_2}\right)\left(\frac{I}{K_I + I}\right) \tag{3.23}$$

Finally, the dynamics of the photobioreactor in Eq. (3.11) was mod-

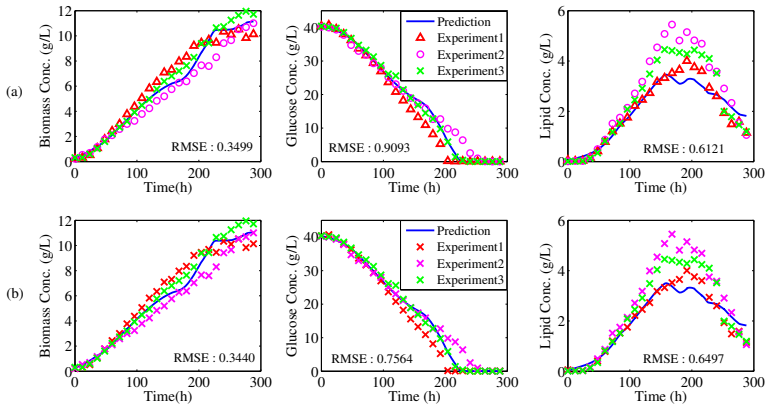

Figure 10: Model tests with and without photoinhibition term ((a) Model without photoinhibition term; (b) Model with photoinhibition term)

ified as follows :

$$\begin{aligned}
\frac{dx}{dt} &= \mu x - xD \\
\frac{dS_1}{dt} &= -\rho x + S_1^i \frac{f_1^i}{V} - S_1 D \\
\frac{dS_2}{dt} &= -\frac{1}{Y_{xs}}\mu x - \frac{1}{Y_l s}\pi x + S_2^i \frac{f_2^i}{V} - S_2 D \\
\frac{dN}{dt} &= \rho x - \mu N - ND \\
\frac{dL}{dt} &= \pi x - \nu L - LD \\
\frac{dV}{dt} &= VD - f_0
\end{aligned} \tag{3.24}$$

Table 1: Results of parameter estimation of the model

Parameter	Value	Unit
Maximum growth rate, μ_m	0.0218	1/h
Minimum nitrogen quota for supporting growth, q_0	0.008	g/g
Minimum lipid quota for supporting growth, l_0	0.001	g/g
Half saturation constant of carbon source for growth, K_{S_2}	0.0008	g/L
Half saturation constant of light for growth, K_I	10.001	$\frac{\mu mol}{m^2 \cdot s}$
Maximum uptake rate, ρ_m	0.071	1/h
Half saturation constant of nitrogen source for uptake, K_{S_1}	0.0003	g/L
Maximum quota of nitrogen above which uptake rate stops, q_m	0.5285	g/g
Maximum lipid production rate, π_m	0.214	1/h
Half saturation constant for oil production, K_π	54.13	g/L
Maximum lipid consumption rate, ν_m	0.0159	1/h
Proportional constant of carbon source for lipid consumption, K_ν	4.947	g/L
Yield coefficient of substrate to biomass, Y_{xs}	1.195	g/g
Yield coefficient of substrate to lipid, Y_{ls}	0.202	g/g

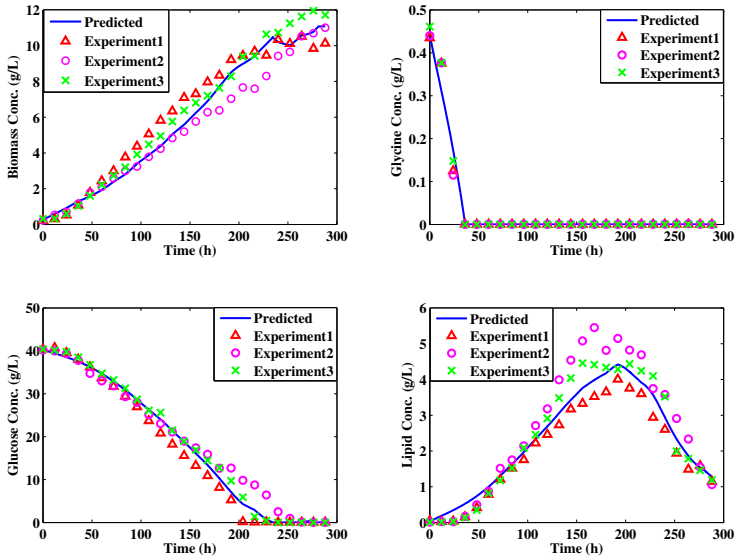

Figure 11: Data fitting of experimental data with the modified photobioreactor model

The model includes 14 parameters, which were estimated using the pattern search tool available in Matlab. Table 1 shows the results of parameter estimation of the model and Fig. 11 shows the results of the simulation data fitted to the experimental. The modified photobioreactor model predicts experimental data more accurately and lipid reduction was also well predicted by the model.

3.6.3 Validation of the model

The modified photobioreactor model with the parameter set estimated in Section 3.6.2 was validated with newly designed experiments. The experiment was designed with different initial concentrations of nutrient (glycine = 1 g/L, glucose = 20 g/L) in the start-up

medium and the optimal input design was calculated with these initial nutrient concentrations and the modified model. Fig. 12 shows the calculated input signals, and the experiment for validation was

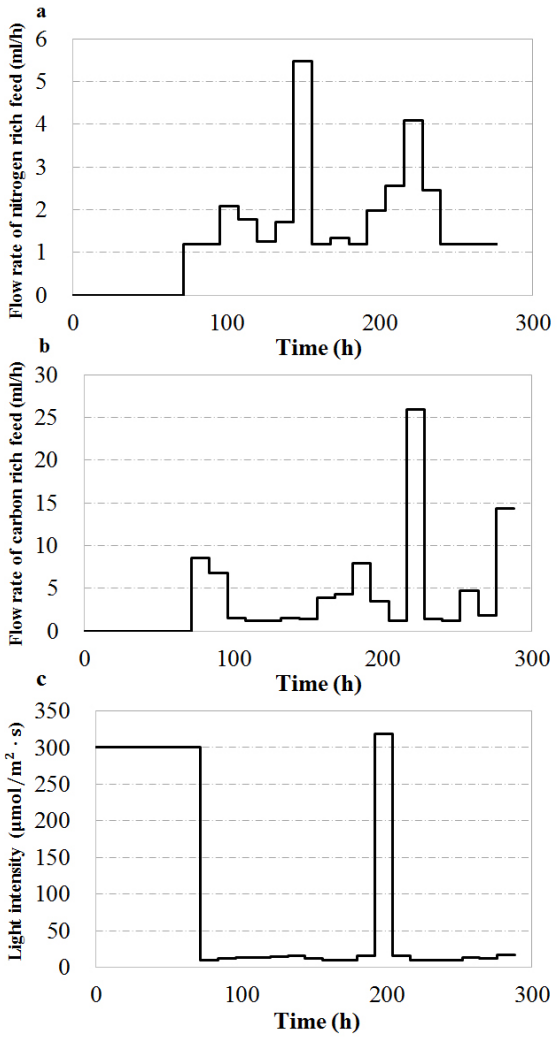

Figure 12: Designed optimal input signals for validation ((a)Flowrate of nitrogen rich feed; (b)Flowrate of carbon rich feed; (c)Light intensity)

performed with these input changes. The results of the validation experiments and model predictions are shown in Fig. 13. Good agreements between model predictions and experimental results within experimental errors were observed in all cases.

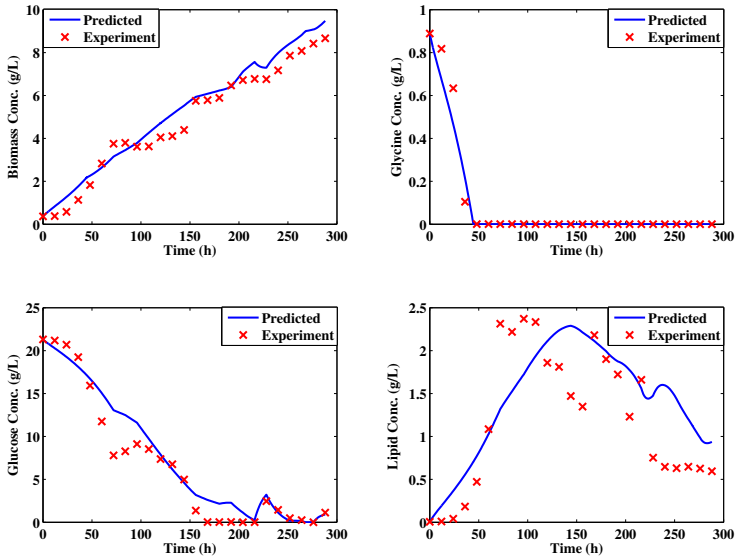

Figure 13: Comparison of model prediction with validation experiments

3.7 Conclusion

The microalgal photobioreactor systems are investigated for developing a mathematical model to predict the productivity of biomass and lipid under mixotrophic conditions. A novel model based on the experimental observations of lipid depletion was proposed with time-varying yield coefficients which reduce the number of parameters. The results of this study suggest that the dynamics of lipid are rela-

tively fast and it is important to cultivate microalgae within the conditions of lipid increase. With its capability of representing various operating scenarios, the proposed model will be useful in a model based control strategy to improve the productivity of biomass and lipid.

Chapter 4

Estimation of lipid concentration

4.1 Introduction

In this chapter, the applicability of various nonlinear estimators for online estimation of the lipid concentration in microalgae cultivation system. Lipid is useful bio-product that has many applications including biofuels and bioactives. Nitrogen deficiency condition reduces the cell growth rate, but increases the amoun of lipid [9, 10]. It is also known that heterotrophic cultivation with glucose as a carbon source significantly enhances the lipid productivity of microalgae [2, 7]. Therefore, it is important to cultivate microalgae within the conditions of maximizing the amount of lipid. Moreover, as the dynamics of lipid are relatively fast, it would have a significant impact on the improvement of lipid productivity if real-time information on lipid concentration can be known [11].

However, improvement of lipid productivity using real-time monitoring and control with experimental validation is limited because measurement of intracellular lipid concentration in microalgae cultivation system is a difficult and time-consuming task with the solvent extraction step involved [18]. In bioreactor systems, on-line measurement of the important variables, such as cell mass, substrate, and

product concentrations is still limited [12]. Many studies have reported on-line measurement of cell counting, optical density, cell size and number, electrical conductivity, pH, and dissolved oxygen for determination of cell mass [38, 39, 40, 41]. Spectroscopy related studies have been proposed for the measurement of substrate concentration such as glucose [42]. However, no lipid sensors exist in the market and there have been no studies on on-line measurement of lipid concentrations.

When some important variables are not available from measurement, soft sensors can give an on-line estimation of the unmeasurable variables or model parameters from more easily-accessible measurements and estimation algorithms [12, 13, 14]. For a linear dynamic system with white system and measurement noises, Kalman filter gives an optimal estimate. However, all practical systems have some degree of nonlinearities and many studies have been proposed for the estimation of nonlinear systems [43, 44, 45]. Comparative studies for nonlinear state estimation using extended Kalman filter (EKF) and unscented Kalman filter (UKF) were reported [46, 44]. Acetate concentration which is not easy to measure was estimated from the easily measurable variables using EKF in $E.\ coli$ cultures [13]. Since the microalgal photobioreactor model is highly nonlinear, this study performed comparative studies on the applicability of EKF, UKF, and particle filter (PF) for estimating the amount of lipid.

In this chapter, estimation of lipid concentrations using on-line measurement of cell mass or glucose concentrations with a photobioreactor model was investigated for various cases. The effects of system noise covariances were tested in case there were model-plant mismatches due to disturbances or parametric mismatches. Then, ap-

propriate types of sensors for lipid estimation were tested. The experimental validations show that UKF and PF with time-varying system noise covariance can improve the performance of lipid estimation.

4.2 Photobioreactor model

Table 2: The parameter values and known quantities of the model

Parameter	Value	Unit
Maximum growth rate, μ_m	0.0582	1/h
Minimum nitrogen quota for supporting growth, q_0	0.0224	g/g
Minimum lipid quota for supporting growth, l_0	0.0976	g/g
Half saturation constant of carbon source for growth, K_{S_2}	0.1002	g/L
Half saturation constant of light for growth, K_I	10.0001	$\frac{\mu mol}{m^2 \cdot s}$
Maximum uptake rate, ρ_m	0.063	1/h
Half saturation constant of nitrogen source for uptake, K_{S_1}	0.00192	g/L
Maximum quota of nitrogen above which uptake rate stops, q_m	0.4997	g/g
Maximum lipid production rate, π_m	0.1328	1/h
Half saturation constant for oil production, K_π	44.217	g/L
Yield coefficient of substrate to biomass, Y_{xs}	0.5262	g/g
Yield coefficient of substrate to lipid, Y_{ls}	0.3417	g/g
Known quantities	Value	Unit
Nitrogen source concentration in inlet feed 1, S_1^i	10	g/L
Carbon source concentration in inlet feed 2, S_2^i	40	g/L

A microalgal photobioreactor model employed in this chapter is summarized in Eq. (4.1). This model is based on the model proposed in chap. 3 [11] with the only difference in the lipid consumption rate which was not used in this study. The model contains 3 inputs, 12 parameters, and 6 system states and Eq. (4.1) represent the mass balance

for the photobioreactor systems.

$$\begin{aligned}
\frac{dx}{dt} &= \mu x - xD \\
\frac{dS_1}{dt} &= -\rho x + S_1^i \frac{f_1^i}{V} - S_1 D \\
\frac{dS_2}{dt} &= -\frac{1}{Y_{xs}}\mu x - \frac{1}{Y_l s}\pi x + S_2^i \frac{f_2^i}{V} - S_2 D \\
\frac{dN}{dt} &= \rho x - \mu N - ND \\
\frac{dL}{dt} &= \pi x - \mu L - LD \\
\frac{dV}{dt} &= f_1^i + f_2^i - f_0
\end{aligned} \tag{4.1}$$

The growth rate (μ), uptake rate (ρ), and lipid production rate (π) were represented in Eq. (4.2).

$$\begin{aligned}
\mu &= \mu_m \left(1 - \frac{q_0}{q}\right)\left(1 - \frac{l_0}{l}\right)\left(\frac{S_2}{K_{S_2} + S_2}\right)\left(\frac{I}{K_I + I}\right) \\
\rho &= \rho_m \left(\frac{S_1}{S_1 + K_{S_1}}\right)\left(\frac{q_m - q}{q_m - q_0}\right) \\
\pi &= \pi_m \left(\frac{S_2}{K_\pi + S_2}\right)\left(1 - \frac{N}{X}\right)\left(1 - \frac{L}{X}\right)
\end{aligned} \tag{4.2}$$

The system inputs are the flow rates of nitrogen feed (f_1^i) and carbon feed (f_2^i) and light intensity (I). D is the dilution rate (ratio of the inlet flow rate to the volume) given by $D = (f_1^i + f_2^i)/V$ and sampling was used as a single source of outlet flow, f_0. S_1^i and S_2^i are the feed concentrations of glycine and glucose, respectively. The parameter values and known quantities used in this chapter are shown in Table 2.

4.3 Estimator algorithms : EKF, UKF, PF

When there are many uncertainties in the process such as model uncertainties, measurement uncertainties, representing the model states using probability density function (pdf) has advantages. State estimation is a means to propagate the pdf of the system states over time in some optimal way. It is most common to use the Gaussian pdf to represent the model state, process and measurement noises. The Gaussian pdf can be characterized by its mean and covariance. The Kalman filter (KF) propagates the mean and covariance of the pdf of the model state in an optimal (minimum mean square error) way in case of linear systems. However, all practical systems posses some degree of nonlinearities and microalgal photobioreactor system in this study is highly nonlinear system. For nonlinear system, the Gaussian pdf for transformed state is not guranted and nonlinear estimator use various ways to represent the pdf for the transformed states.

4.3.1 Extended Kalman Filter (EKF)

Extended Kalman filter (EKF) is the most widely used nonlinear state estimation technique. The EKF estimates the state in Eq. (4.3) by using a linearized model and Kalman filter algorithm at each sample time.

$$\begin{aligned} \dot{z}(t) &= f(z(t), u(t)) + w(t) \\ y(t) &= h(z(t)) + v(t) \end{aligned} \tag{4.3}$$

where z is the state vector, y is the measurement, w is the system noise, v is the measurement noise. The system and measurement

noises are assumed to have independent random Gaussian noises with zero mean and covariances Q and R, respectively.

By linearization of the first order approximation of Eq. (4.3), the linearized model can be obtained and after discretization of the continuous linearized model, discrete time linear state-space form can be obtained as follows :

$$\begin{aligned} z_{k+1} &= A_k z_k + B_k u_k + w_k \\ y_k &= C_k z_k + v_k \end{aligned} \tag{4.4}$$

Then, EKF algorithm can be summarized as the following steps.

Predict a priori state estimate and error covariance :

$$\begin{aligned} \hat{z}_k^- &= f(\hat{z}_{k-1}, u_{k-1}) \\ P_k^- &= A_{k-1} P_{k-1} A_{k-1}^T + Q \end{aligned} \tag{4.5}$$

where $\hat{z}^-$ means priori estimated value and P is error covariance. Calculate the Kalman filter gain :

$$K_k = P_k^- C_k^T (C_k P_k^- C_k^T + R)^{-1} \tag{4.6}$$

A posteriori state estimate and error covariance (measurement update) :

$$\begin{aligned} \hat{z}_k &= \hat{z}_k^- + K_k(y_k - h(\hat{z}_k^-)) \\ P_k &= P_k^- - K_k C_k P_k^- \end{aligned} \tag{4.7}$$

The main disadvantages of EKF includes : (i) approximated linear

model can be inaccurate for highly nonlinear cases, in which estimate may fail to converge to the true state; (ii) update of covariance needs calculation of Jacobian matrices, which can be cumbersome and (iii) constraints are not considered in th algorithm.

4.3.2 Unscented Kalman Filter (UKF)

UKF was suggested as an alternative to EKF. It uses a sample-based approach to obtaining mean and covariance of transformed data. UKF generates a set of deterministic vectors called sigma points which have a minimal set of sample points with known values of mean $\bar{z}$ and covariance P. UKF is based on the premise that the mean and covariance of transformed sigma points is similar to the mean and covariance of true value y.

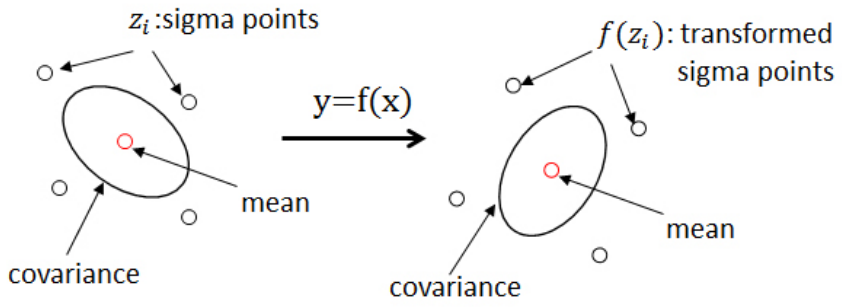

Figure 14: Transformation of sigma points

The UKF algorithm is summarized as follows [47] :
Calculate $2n + 1$ sigma points $z^{(i)}$ and weight W : sigma points are calculated to satisfy cases where mean and covariance are equal to $\bar{z}$

and P.

$$
\begin{aligned}
z_{k-1}^{(1)} &= \bar{z}_{k-1}, \qquad W^{(1)} = \frac{\kappa}{n+\kappa} \\
z_{k-1}^{(i+1)} &= \bar{z}_{k-1} + \tilde{z}^{(i)},\ W^{(i+1)} = \frac{1}{2(n+\kappa)} \quad i = 1, \cdots, 2n \\
\tilde{z}^{(i)} &= \left(\sqrt{(n+\kappa)P_{k-1}}\right)_i^T \qquad i = 1, \cdots, n \\
\tilde{z}^{(n+i)} &= -\left(\sqrt{(n+\kappa)P_{k-1}}\right)_i^T \qquad i = 1, \cdots, n
\end{aligned}
\tag{4.8}
$$

where n is the size of vector z, κ is arbitrary constant, $\sqrt{nP}$ is the matrix square root of nP such that $(\sqrt{nP})^T\sqrt{nP} = nP$. Predict a priori state estimate and error covariance :

$$
\begin{aligned}
z_k^{(i)} &= f(z_{k-1}^{(i)}, u_{k-1}) \\
\hat{z}_k^- &= \sum_{i=1}^{2n+1} W^{(i)} \hat{z}_k^{(i)} \\
P_k^- &= \sum_{i=1}^{2n+1} W^{(i)} (z_k^{(i)} - \hat{z}_k^-)(z_k^{(i)} - \hat{z}_k^-)^T + Q
\end{aligned}
\tag{4.9}
$$

where $\hat{z}$ means estimated value and $\hat{z}^-$ means priori estimated value. Re-calculation of sigma points using current state estimate and error covariance : (same with Eq. (4.8))

A posteriori state estimate and error covariance (measurement up-

date) :

$$
\begin{aligned}
y_k^{(i)} &= h(z_k^{(i)}) \\
\hat{y}_k &= \sum_{i=1}^{2n+1} W^{(i)} y_k^{(i)} \\
P_y &= \sum_{i=1}^{2n+1} W^{(i)} (y_k^{(i)} - \hat{y}_k)(y_k^{(i)} - \hat{y}_k)^T + R \\
P_{zy} &= \sum_{i=1}^{2n+1} W^{(i)} (z_k^{(i)} - \hat{z}_k^-)(y_k^{(i)} - \hat{y}_k)^T \\
K_k &= P_{zy} P_y^{-1} \\
\hat{z}_k &= \hat{z}_k^- + K_k (y_k - \hat{y}_k) \\
P_k &= P_k^- - K_k P_y K_k^T
\end{aligned}
\tag{4.10}
$$

The UKF propagates the pdf in a simple and effective way and it is accurate up to second order in estimating mean and covariance.

4.3.3 Particle Filter (PF)

The important assumption underlying Kalman filter is that it follows the Gaussian distribution. In a Gaussian system, the mean and covariance of estimate are enough for complete description of the distribution. However, for non-Gaussian systems, if an entire probability distribution of the state is available, then it can be informative. One technique that can provide such information is PF and it is based on the sequential Monte-carlo sampling approach. The PF algorithms are summarized in the following steps [47].
Generate particles : randomly generate N particles based on the initial probability density function of $p(z_0)$.

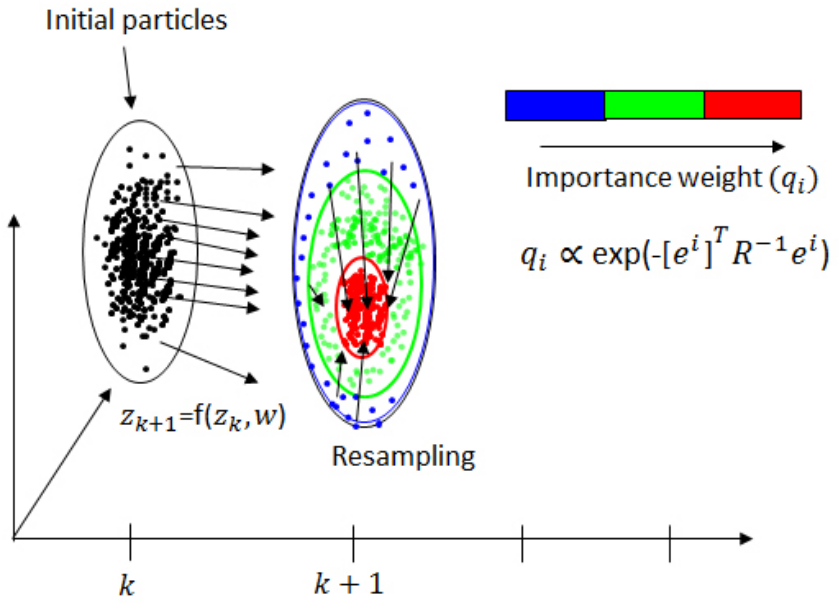

Figure 15: Transformation of particles

Calculate a priori particles :

$$z^-_{k,i} = f(z_{k-1,i}, u_{k-1}) + w_{k-1} \qquad (i = i, \cdots, N) \tag{4.11}$$

Calculate relative likelihood of each particles (q_i):

$$\begin{aligned} q_i &= P[(y_k = y^*)|(z_k = z^-_{k,i})] \\ &= P[v_k = y^* - h(z^-_{k,i})] \\ &\approx \frac{1}{(2\pi)^{m/2}\,|R|^{1/2}} exp\left(\frac{-[y^* - h(z^-_{k,i})]^T R^{-1}[y^* - h(z^-_{k,i})]}{2}\right) \end{aligned} \tag{4.12}$$

where y^* is the measurement data.
Normalize the relative likelihood obtained in Eq. (4.12) :

$$q_i = \frac{q_i}{\sum_{j=1}^{N} q_j} \tag{4.13}$$

Generate a set of a posteriori particles,$z_{k,i}$ (resampling step) :
1. Generate random number r that is uniformly distributed on [0,1].
2. Accumulate the likelihoods q_i into a sum until it is greater than r.
$\sum_{m=1}^{j-1} q_m < r$, $\sum_{m=1}^{j} q_m \geq r$, then,

$$z_{k,i} = z_{k,j}^{-} \tag{4.14}$$

with the probability of $q_j (i, j = 1, \cdots, N)$

Finally, resampled particles, $z_{k,i}$ are distributed according to the pdf $p(x_k|y_k)$ and can compute any desired statistical measure of this pdf. We typically are most interested in computing the mean and the covariance.

4.4 Simulation studies

For the estimation of lipid concentration in microalgal photobioreactor system, four cases were tested to determine suitable estimators and types of sensors for various system noises. When designing estimator, determination of system noise covariance (Q) and measurement noise covariance (R) is important for improving estimator performance. For the measurement noise, it can be easily determined from the sensor characteristics. However, it is not easy to characterize the system noise. To investigate the effect of system noise covari-

ance on the estimator performance, two different system noise cases were tested in the first case study. In addition, to compare the estimator performances for plant-model mismatches, two simulation cases were tested. In the second case, the true system was assumed to be different from the model owing to disturbances during cultivation. In the third case, it was assumed that some parameter values were different from the initial known values due to unknown metabolic reactions. Finally, to find appropriate sensors and equipments for lipid estimates, various scenarios were simulated in the fourth case.

During the simulations, the following conditions and assumptions were applied in all the case studies.

(a) The three input variables were provided as in Fig. 7.

(b) The term 'true system' means the mathematical model perfectly describing the system. The mismatch between the true system and model in use comes from various reasons such as system and measurement noise, disturbances, and unknown reactions.

(c) The state variables of the photobioreactor model consist of five concentrations and a volume of culture media, which have non-negative values. To handle non-negative constraints of the state variables, absolute values were used for the true system values in case noise term was added as in Eq. (4.15).

$$\begin{aligned} z_{k+1} &= |f(z_k, u_k) + w_k| \\ y_k &= |h(z_k) + v_k| \end{aligned} \tag{4.15}$$

For the estimator, UKF and PF algorithms were modified to give non-negative constraints. In case of UKF, absolute values were applied to

the sigma points of Eq. (4.8) and modified as in Eq. (4.16).

$$\hat{z}_{k-1}^{(i+1)} = |\bar{z}_{k-1} + \tilde{z}^{(i)}|,\ i = 1, \cdots, 2n \tag{4.16}$$

In case of PF, absolute values were taken in two steps. First, when generating particles, absolute values were taken to the N particles. Then, absolute values of a priori particles of Eq. (4.11) were used as in Eq. (4.17).

$$z_{k,i}^{-} = |f(z_{k-1,i}, u_{k-1}) + w_{k-1}| \qquad (i = i, \cdots, N) \tag{4.17}$$

(d) Initial estimate value was assumed to have 10% difference with the true initial value.
(e) The number of particles used in PF was 100.

4.4.1 Case study 1 : effect of system noise covariance (Q)

When designing an estimator, system noise covariance is used to reflect confidence in the system dynamics and balance between model predictions and measurements. If the model is accurate, the small system noise covariance can be used to give more weight to model values. On the other hand, a large system noise covariance can give more weight to measurement values for a less accurate model. In this case study, simulations were tested with two different system noise covariance values. The first case assumed the model matches the true system well with a small system noise covariance and the second case gives large system noise covariances to reflect uncertainties in the system. In both cases, biomass and glucose sensor data

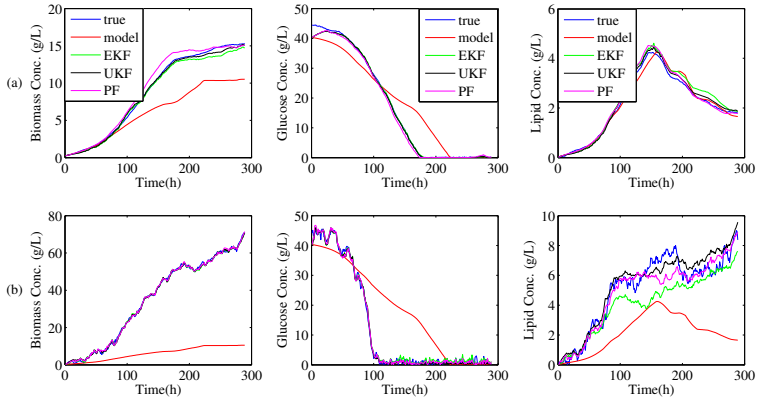

Figure 16: Simulation results of various system noise covariance values ((a) $Q = \mathrm{diag}([0.01^2, 0.01^2, 0.1^2, 0.01^2, 0.01^2, 0.01^2])$; (b) $Q = \mathrm{diag}([0.5^2, 0.1^2, 1^2, 0.1^2, 0.2^2, 0.01^2])$)

were assumed to be used as measurements, and measurement noise covariance (R) was assumed to be $R = \mathrm{diag}([1.5^2, 1.5^2])$. In this case study, same noise covariances were used in the true system with an estimator. The covariances of the two cases are as follows :

(a) $Q = \mathrm{diag}([0.01^2, 0.01^2, 0.1^2, 0.01^2, 0.01^2, 0.01^2])$

(b) $Q = \mathrm{diag}([0.5^2, 0.1^2, 1^2, 0.1^2, 0.2^2, 0.01^2])$

Simulation results of the two different cases are shown in Fig. 16. For measured variables (biomass, glucose) all estimators show good performances in tracking true values in both cases. However, for unmeasured variables (lipid), there were some discrepancies in the performance of estimators. When large system noise was added, EKF shows the worst. Since EKF is based on a linearized model for every sample time point, tracking true values for a highly nonlinear system with large noise is still difficult using EKF.

4.4.2 Case study 2 : effect of disturbances

In this case study, the effect of disturbances on estimator performances with various system noise covariances were investigated. In microalgae cultivation system, the flow rates of nitrogen feed (f_1^i) and carbon feed (f_2^i) are used as input variables and these two feeds are supplied from the stock solutions. In this case study, it was assumed that the concentrations of these stock solutions were abruptly changed by some mistake of the operator. The concentration of the stock solution of feed 1 (S_1^i) and feed 2 (S_2^i) were changed to 20 g/L and 60 g/L from 10 g/L and 40 g/L after 72 h, respectively. The true system data were generated using the changed concentrations of stock solutions without system noise.

Simulations were tested with three different system noise covariances. Especially, to reflect the noise characteristics of the microalgae cultivation system, time-varying system noise covariances were introduced. In real system, as microalgae grow, unknown metabolic reactions or phenomena make systems have more uncertainties as time goes by. In such case, it was assumed that system noise covariances of state variables related to the product (x, N, L) are increased proportional to the amounts produced and system noise covariances of state variables related to substrate (S_1, S_2) are increased proportional to the amounts consumed. However, when the substrates were almost consumed, system noise covariances have small values. This is because when the values approach to zero, consumption of substrates also decreased, which does not follow the above assumption. Considering these points, system noise covariances were generated as follows :
(1) At each time step, calculate Δz_k, which represent produced or

consumed amount of each state variables.

$$\Delta z_k = \begin{array}{ll} |z_k - z_0| & (for\ all\ state) \\ z_k & (for\ S_1\ and\ S_2\ ,\ if\ z_k \leq 0.1 \times z_0) \end{array} \tag{4.18}$$

(2) Generate three points (Δz_k, $\pm 10\%$ of Δz_k) to represent proportional distribution to the produced or consumed amount and calculate variances (V_k) of each three point (Z_i=[Δz_k, $0.9\Delta z_k$, $1.1\Delta z_k$]).

$$V_k = \frac{1}{n-1}\sum_{i=1}^{n}(Z_i - \Delta z_k)^2,\ n = 3 \tag{4.19}$$

(3) Calculate Q_k as in Eq. (4.23).

$$Q_k = \alpha \times \mathrm{diag}(\mathrm{V_k}) \tag{4.20}$$

where α is a design parameter for time-varying system noise covariances to reflect the rate which is proportional to produced or consumed amount of states. The advantage of using Eq. (4.23) is that it reflects the noise characteristics of microalgal cultivation system more accurately while considering time-varying value. Furthermore, it only requires one parameter α while previous methods need to determine six system noise covariances, usually by trial-and-errors corresponding to each state variable.

The covariances of the three cases are summarized as follows :

(a) $Q = \mathrm{diag}([0.07^2, 0.05^2, 0.7^2, 0.02^2, 0.03^2, 0.01^2])$

(b) $Q = \mathrm{diag}([0.5^2, 0.1^2, 1^2, 0.1^2, 0.2^2, 0.01^2])$

(c) Time-varying Q with α=0.05

In all three cases, biomass and glucose sensor data were assumed to

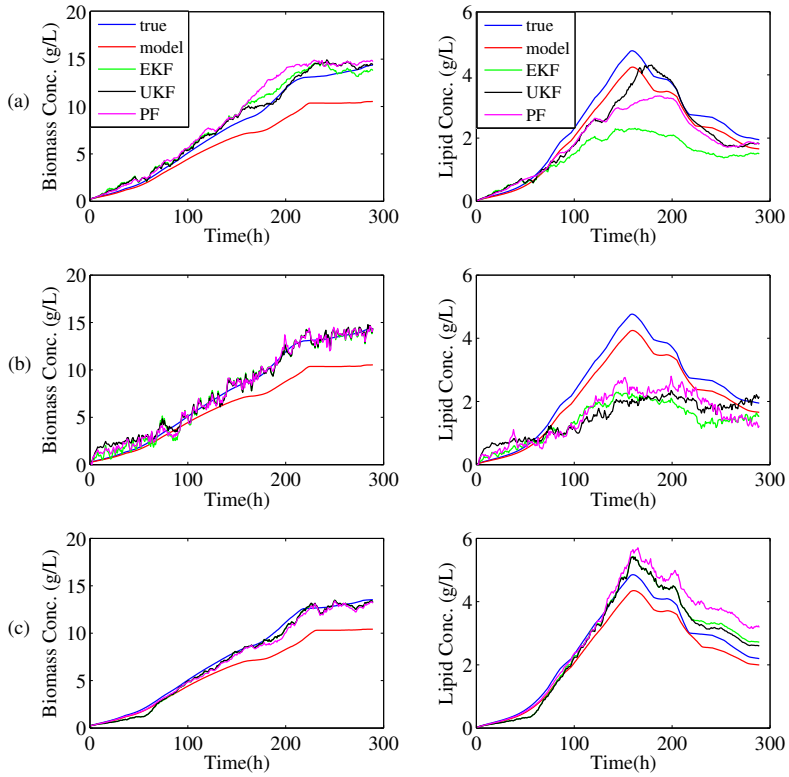

Figure 17: Simulation results of various system noise covariance with disturbances in the system ((a) $Q = \mathrm{diag}([0.07^2, 0.05^2, 0.7^2, 0.02^2, 0.03^2, 0.01^2])$; (b) $Q = \mathrm{diag}([0.5^2, 0.1^2, 1^2, 0.1^2, 0.2^2, 0.01^2])$; (c) Time-varying values of Q with α=0.05)

be used as measurements with $R = \mathrm{diag}([1.5^2, 1.5^2])$.

Simulation results are shown in Fig. 15. The biomass plot in Fig. 17, (a) show that despite using an adequate size for the system noise covariance of estimator, the estimator could not track the true system satisfactorily. To give more weight to the measurement data, larger system noise covariance was used in case (b). Fig. 17, (b) shows that

biomass data were satisfactorily tracked by the estimator, but in this case, lipid estimates differed significantly from the true system. Finally, when time-varying Q with α=0.05 was applied, the estimator can track the true system value of biomass and lipid satisfactorily, with the exception of EKF as shown in Fig. 17, (c).

4.4.3 Case study 3: effect of parametric mismatches

In this case study, it was assumed that the values of some model parameters differed from initial known values as a result of unknown metabolic reactions. It was assumed that μ_m and K_{S_2} of the true system have different values with the model. The true system has 0.028 for μ_m and 0.30 for K_{S_2} instead of 0.0582 and 0.1002, respectively. Other conditions were kept the same as for case study 2.

Simulation results are shown in Fig. 18. It was observed that the true system and model have large differences especially with respect to lipid concentration. When system noise covariance in case (a) was applied, the true system of biomass could not be estimated satisfactorily. When system noise covariance was increased to give more weight to measurement data, the biomass data could be tracked. However, increasing system noise covariance gave poorer estimation performances for the unmeasured variable, lipid, as shown in Fig. 18. (b). However, when time-varying values of Q with α=0.05 was applied, the estimation performance was improved especially for the lipid concentration.

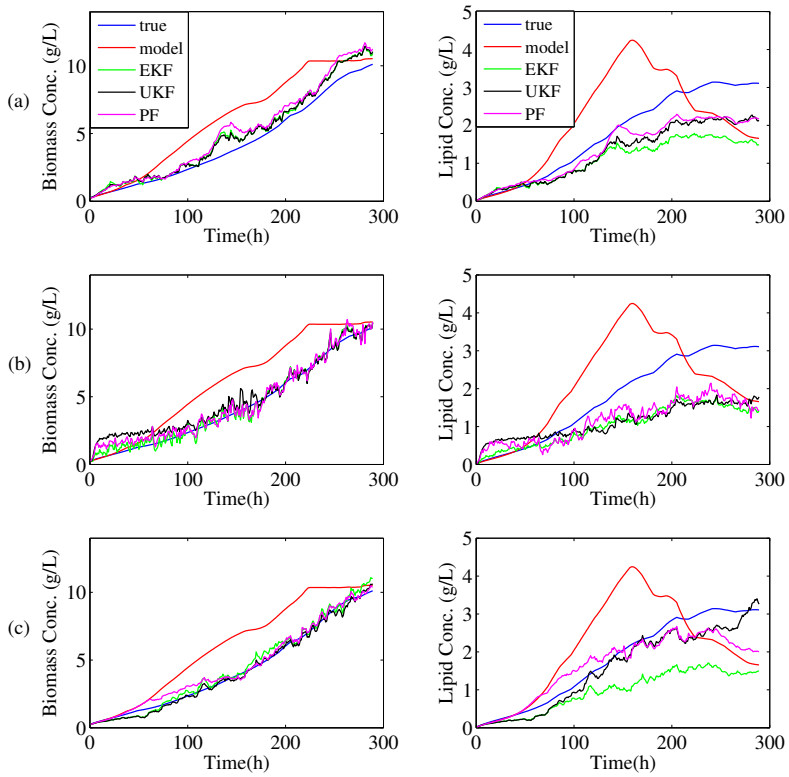

Figure 18: Simulation results of various system noise covariance with parametric mismatches in the system ((a) $Q = \mathrm{diag}([0.07^2, 0.05^2, 0.7^2, 0.02^2, 0.03^2, 0.01^2])$; (b) $Q = \mathrm{diag}([0.5^2, 0.1^2, 1^2, 0.1^2, 0.2^2, 0.01^2])$;; (c) Time-varying values of Q with α=0.05)

4.4.4 Case study 4 : types of equipments

To determine appropriate sensors and equipment for lipid estimation, various scenarios were simulated. In this case study, system noise covariance was assumed to be $Q = \mathrm{diag}([0.07^2, 0.05^2, 0.7^2, 0.02^2, 0.03^2, 0.01^2])$ and the same system and measurement noise

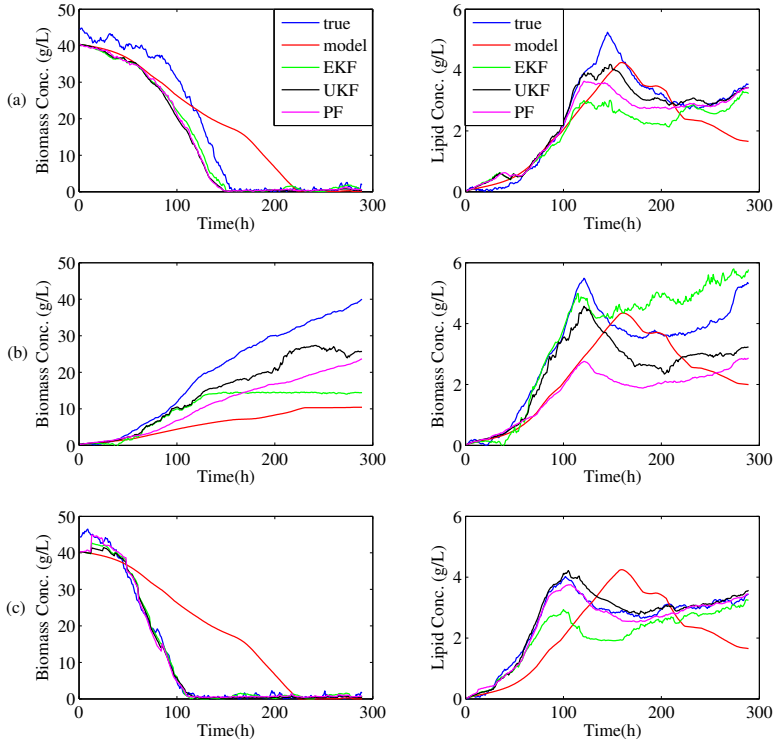

Figure 19: Comparison of estimator performance with applying different tyupes of sensors or equipment ((a) only biomass sensor data ($R = 1.5^2$); (b) only glucose sensor data ($R = 1.5^2$); (c) biomass sensor data, glucose lab data (data obtained every 12 hr, $R = 0.5^2$))

covariances were assumed to be used for the true system and the estimator. Three different cases (the number of equipment and types) were compared :

(a) biomass sensor data only ($R = 1.5^2$)

(b) glucose sensor data only ($R = 1.5^2$)

(c) biomass sensor data and glucose lab data (data obtained every 12

hr, $R = 0.5^2$)

Simulation results of the three different cases are shown in Fig. 19. For graphical clarity, measured data which were well estimated in each case are omitted in the figure. Among all three cases, when only glucose sensor was used as a measurement, as in case (b), the estimator showed worst performances in estimating both biomass and lipid. Therefore, it is not appropriate to use only glucose sensor for estimation purposes. When only biomass sensor was used as a measurement, it showed better estimation performance than glucose sensor only, however, there were some differences from the true system values. In a real system, biomass data are easier to obtain from various sensors compared to glucose sensor data. For situations where a glucose sensor was unavailable, infrequent sampled laboratory data were tested in case (c) to confirm whether it could improve the estimator performance. As shown in Fig. 19. (c), glucose data were corrected compared with case (a) and estimation performances were improved.

Considering all case studies, lipid estimates using EKF showed a large difference with the true system values. Therefore, EKF is not appropriate for lipid estimation in photobioreactor systems. Overall, UKF and PF show satisfactory estimation performances in most of the cases. In particular, biomass sensor with infrequent glucose lab data can improve the estimation performance. Therefore, experimental validation was performed with these types of measurements.

4.5 Experimental results

$C\ protothecoides$ were cultivated in a photobioreactor using the inputs shown in Fig. 7 to investigate whether the estimator can be

applied in estimating lipid concentration as studied in the simulation cases. During the cultivation, biomass data from the turbidity sensor and glucose data from analysis of the sampled microalgae using HPLC were obtained and used as measurement sources for lipid estimation. Using the experimental data, performance of the estimators was tested with two different cases. The two cases are summarized as follows :

(a) biomass sensor data, glucose lab data (data obtained every 12 hr, $R = 0.5^2$), $Q = \mathrm{diag}([0.5^2, 0.1^2, 1^2, 0.1^2, 0.2^2, 0.5^2])$

(b) biomass sensor data, glucose lab data (data obtained every 12 hr, $R = 0.5^2$), time-varying values of Q with α=0.25

The reason for employing the above system noise covariance values in (a) is that smaller Q values cannot estimate experimental data satisfactorily. The simulation and experimental results are shown in Fig. 20. When comparing the fixed noise covariance with the time-varying noise covariance, time-varying noise covariance was much more effective for the estimation of lipid concentration. Furthermore, time-varying system noise covariance also improved the estimation peroformances of biomass and glucose concentrations. Overall, biomass sensor with infrequent glucose lab data could improve the estimator performance. UKF and PF demonstrated satisfactory performances in the estimation of lipid concentration compared to EKF.

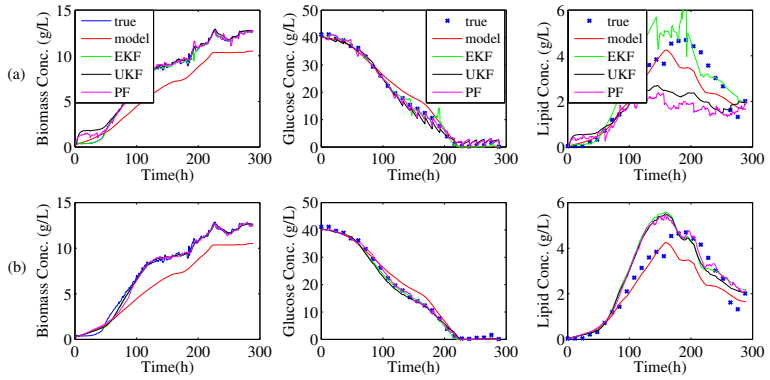

Figure 20: Validation of estimator performance with experimental data ((a) biomass sensor data, glucose lab data (data obtained every 12 hr, $R = 0.5^2$), $Q = \text{diag}([0.5^2, 0.1^2, 1^2, 0.1^2, 0.2^2, 0.01^2])$; (b) biomass sensor data, glucose lab data (data obtained every 12 hr, $R = 0.5^2$), time-varying values of Q with α=0.25)

4.6 Conclusions

Estimation of lipid concentration in microalgal photobioreactor system was studied. It was found that EKF was not suitable for estimating lipid concentration in most cases while UKF and PF showed satisfactory performances. Finally, experimental validation was performed that suggested time-varying system noise covariance with a biomass sensor and infrequent glucose lab data can improve the estimation performance significantly. However, there are some limitations in applying this method that model has to be accurate for estimating unmeasured variables. If the model is not accurate, parameter update by estimation of key parameters is one way to enhance the robustness of the estimator.

Chapter 5

Optimization

5.1 Introduction

In this chapter, various optimization methods were investigated in microalgal photobioreactor system to maximize the biomass and lipid concentration. There are many efforts to improve the growth rate or lipid contents of microalgal cells in the fields of process optimization, metabolic engineering, and genetic engineering [48, 49, 50, 51, 52, 53] . Among them, this study is focused on the process optimization using model predictive control for the improvement of biomass and lipid productivity.

In order to maximize the productivity of biomass and lipid, advanced control strategies might be promising tools to improve the performance of microalgal photobioreactor systems [50, 54]. However, there are some difficulties in applying model-based control strategies to microalgal cultivation systems. Microalgae cultivation systems are network of complex biochemical reactions manipulated by enzyme kinetics [55, 56]. Modelling of these complex biological systems accurately is difficult task since metabolism inside the cells makes systems states and parameters have uncertainties [54, 57]. Moreover, on-line measurement of important variables such as cell mass, sub-

strate, and product concentration is still limited [12]. Especially, no lipid sensors exist in the market. Recently, some studies have been proposed to maximize the biomass and lipid productivities using advanced control strategies. Interior point optimization and model predictive control along with moving horizon estimator are proposed to maximize and regulate lipid production in heterotrophic microalgae cultivation [54]. An adpative, non-linear model based strategy, in which model parameters are re-estimated based on the newly available data is also proposed [57]. In both studies, biomass and lipid productivities are improved significantly. However, both studies are not validated with experimental data.

In this chapter, optimization of microalgal photobioreactor with $Chlorella\ protothecoides$ as a strain was investigated with experimental validation for the improvement of biomass and lipid productivity. Lipid concentration was estimated using uncented Kalman filter (UKF) which is non-linear estimator to employ it as lipid data for model predictive control (MPC) [58]. From the experimental results, MPC can improve the productivity of biomass and lipid significantly. However, when suddenly large amount of inputs are introduced to the photobioreactor, unexpected phenomena like lag phase was occured, which needs more studies for optimization of algal production.

5.2 Microalgal photobioreactor model

A microalgal photobioreactor model employed in this chapter is summarized in Eq. (5.1). This model is based on the model proposed in chap. 4.2 with the only difference in the lipid production rate. This

model composed of 3 inputs, 13 parameters, and 6 system states.

$$\begin{aligned}
\frac{dx}{dt} &= \mu x - xD \\
\frac{dS_1}{dt} &= -\rho x + S_1^i \frac{f_1^i}{V} - S_1 D \\
\frac{dS_2}{dt} &= -\frac{1}{Y_{xs}}\mu x - \frac{1}{Y_l s}\pi x + S_2^i \frac{f_2^i}{V} - S_2 D \\
\frac{dN}{dt} &= \rho x - \mu N - ND \\
\frac{dL}{dt} &= \pi x - \mu L - LD \\
\frac{dV}{dt} &= f_1^i + f_2^i - f_0
\end{aligned} \tag{5.1}$$

The growth rate (μ), uptake rate (ρ), and lipid production rate (π) were represented in Eq. (5.2).

$$\begin{aligned}
\mu &= \mu_m \left(1 - \frac{q_0}{q}\right)\left(1 - \frac{l_0}{l}\right)\left(\frac{S_2}{K_{S_2} + S_2}\right)\left(\frac{I}{K_I + I}\right) \\
\rho &= \rho_m \left(\frac{S_1}{S_1 + K_{S_1}}\right)\left(\frac{q_m - q}{q_m - q_0}\right) \\
\pi &= \pi_m \left(\frac{S_2}{K_\pi + S_2}\right)\left(1 - \frac{N}{X}\right)\left(\frac{l_m - l}{l_m}\right)
\end{aligned} \tag{5.2}$$

For the model proposed in chap. 4, it was observed that in specific conditions for maximizing the lipid productivity, lipid content significantly increased that it does not reflect real phenomena. To prevent unrealistic lipid quota increase, maximum quota of lipid (l_m) was assumed in lipid production rate (π).

The system inputs are the flow rates of nitrogen feed (f_1^i) and carbon feed (f_2^i) and light intensity (I). D is the dilution rate (ratio of the inlet flow rate to the volume) given by $D = (f_1^i + f_2^i)/V$ and

sampling was used as a single source of outlet flow, f_0. S_1^i and S_2^i are the feed concentrations of glycine and glucose, respectively. The parameter values and known quantities are shown in Table 3.

Table 3: The parameter values and known quantities of the model

Parameter	Value	Unit
Maximum growth rate, μ_m	0.0418	1/h
Minimum nitrogen quota for supporting growth, q_0	0.0196	g/g
Minimum lipid quota for supporting growth, l_0	0.0006	g/g
Half saturation constant of glucose for growth, K_{S_2}	0.1002	g/L
Half saturation constant of light for growth, K_I	66.5337	$\frac{\mu mol}{m^2 \cdot s}$
Maximum uptake rate, ρ_m	0.1197	1/h
Half saturation constant of glycine for uptake, K_{S_1}	0.5793	g/L
Maximum quota of nitrogen above which uptake rate stops, q_m	0.2109	g/g
Maximum lipid production rate, π_m	0.0762	1/h
Half saturation constant for oil production, K_π	12.5596	g/L
Maximum quota of lipid above which lipid production stops, l_m	0.6995	g/g
Yield coefficient of glucose to active biomass, Y_{xs}	0.9597	g/g
Yield coefficient of glucose to lipid, Y_{ls}	0.1908	g/g
Known quantities	Value	Unit
Glycine concentration in inlet feed 1, S_1^i	10	g/L
Glucose concentration in inlet feed 2, S_2^i	200	g/L

5.3 State estimation

For the estimation of lipid concentration in microalgal photobioreactor system, unscented Kalman filter (UKF) and particle filter (PF) with time-varying system noise covariance show good performances in chapter 4 [58]. From that results, UKF was used for the estimation of lipid concentration in this chapter.

The UKF estimates the state in Eq. (5.3) by using the model

with a sample based approach to obtaining mean and covariance of transformed data.

$$\begin{aligned} \dot{z}(t) &= f(z(t), u(t)) + w(t) \\ y(t) &= h(z(t)) + v(t) \end{aligned} \tag{5.3}$$

where z is the state vector, y is the measurement, w is the system noise, v is the measurement noise. The system and measurement noises are assumed to have independent random gaussian noises with zero mean and covariances Q and R, respectively.

UKF generates a set of deterministic vectors called sigma points which have a minimal set of sample points with known values of mean $\bar{z}$ and covariance P. UKF is based on the premise that the mean and covariance of transformed sigma points is similar to the mean and covariance of true value y. The UKF algorithm is summarized as follows [47] :
Calculate $2n + 1$ sigma points $z^{(i)}$ and weight W : sigma points are calculated to satisfy cases where mean and covariance are equal to $\bar{z}$ and P.

$$\begin{aligned} z_{k-1}^{(1)} &= \bar{z}_{k-1}, \qquad W^{(1)} = \frac{\kappa}{n+\kappa} \\ z_{k-1}^{(i+1)} &= \bar{z}_{k-1} + \tilde{z}^{(i)},\ W^{(i+1)} = \frac{1}{2(n+\kappa)} \quad i = 1, \cdots, 2n \\ \tilde{z}^{(i)} &= \left(\sqrt{(n+\kappa)P_{k-1}}\right)_i^T \qquad i = 1, \cdots, n \\ \tilde{z}^{(n+i)} &= -\left(\sqrt{(n+\kappa)P_{k-1}}\right)_i^T \qquad i = 1, \cdots, n \end{aligned} \tag{5.4}$$

where n is the size of vector z, κ is arbitrary constant, $\sqrt{nP}$ is the matrix square root of nP such that $(\sqrt{nP})^T\sqrt{nP} = nP$.

Predict a priori state estimate and error covariance :

$$
\begin{aligned}
z_k^{(i)} &= f(z_{k-1}^{(i)}, u_{k-1}) \\
\hat{z}_k^- &= \sum_{i=1}^{2n+1} W^{(i)} \hat{z}_k^{(i)} \\
P_k^- &= \sum_{i=1}^{2n+1} W^{(i)} (z_k^{(i)} - \hat{z}_k^-)(z_k^{(i)} - \hat{z}_k^-)^T + Q
\end{aligned}
\tag{5.5}
$$

where $\hat{z}$ means estimated value and $\hat{z}^-$ means priori estimated value. Re-calculation of sigma points using current state estimate and error covariance : (same with Eq. (5.4))
A posteriori state estimate and error covariance (measurement update) :

$$
\begin{aligned}
y_k^{(i)} &= h(z_k^{(i)}) \\
\hat{y}_k &= \sum_{i=1}^{2n+1} W^{(i)} y_k^{(i)} \\
P_y &= \sum_{i=1}^{2n+1} W^{(i)} (y_k^{(i)} - \hat{y}_k)(y_k^{(i)} - \hat{y}_k)^T + R \\
P_{zy} &= \sum_{i=1}^{2n+1} W^{(i)} (z_k^{(i)} - \hat{z}_k^-)(y_k^{(i)} - \hat{y}_k)^T \\
K_k &= P_{zy} P_y^{-1} \\
\hat{z}_k &= \hat{z}_k^- + K_k (y_k - \hat{y}_k) \\
P_k &= P_k^- - K_k P_y K_k^T
\end{aligned}
\tag{5.6}
$$

In this study, to reflect the noise characteristics of the microalgae cultivation system, time-varying system noise covariances in chap. 4 were introduced. In real system, as microalgae grow, unknown metabolic

reactions or phenomena make systems have more uncertainties as time goes by. In such case, it was assumed that system noise covariances of state variables related to the product (x, N, L) are increased proportional to the produced amounts of products and system noise covariances of state variables related to substrate (S_1, S_2) are increased proportional to the consumed amounts of substrates. However, when the substrates were almost consumed, system noise covariances have small values. This is because when the values approach to zero, consumption of substrates also decreased, which does not follow the above assumption. Considering these points, system noise covariances were generated as follows :

1) At each time step, calculate Δz_k, which represent produced or consumed amounts of each state variables.

$$\Delta z_k = \begin{array}{ll} |z_k - z_0| & (for\ all\ state) \\ z_k & (for\ S_1\ and\ S_2\ ,\ if\ z_k \leq 0.1 \times z_0) \end{array} \tag{5.7}$$

2) Generate three points (Δz_k, $\pm 10\%$ of Δz_k) to represent proportional distribution to the produced or consumed amount and calculate variances (V_k) of each three point (Z_i=[Δz_k, $0.9\Delta z_k$, $1.1\Delta z_k$]).

$$V_k = \frac{1}{n-1} \sum_{i=1}^{n} (Z_i - \Delta z_k)^2,\ n = 3 \tag{5.8}$$

3) Calculate Q_k as in Eq. (5.9).

$$Q_k = \alpha \times \mathrm{diag}(\mathrm{V_k}) \tag{5.9}$$

where α is a design parameter for time-varying system noise covari-

ances to reflect the rate which is proportional to produced or consumed amount of states. The advantage of using Eq. (5.9) is that it reflects the noise characteristics of microalgal cultivation system more accurately while considering time-varying value.

5.4 Optimization

5.4.1 Manual operation based on algal growth characteristic

For the maximizing the biomass and lipid production in photobioreactor system, microalgae were cultivated with various optimization method. At first, microalgae were cultivated based on author's experience. Generally, it was known that nitrogen dificiency condition reduces the cell growth rate, but increases the amount of lipid. Reflecting this point, nitrogen feed was supplied from the beginning to the middle of the cultivation process while carbon source feed was supplied whole the cultivation process as in Fig. 21, (a). The intention of this is to stimulate the growth of microalgae initially and then to convert it to the lipid components.

5.4.2 Open-loop optimization

Sencondly, open-loop optimization was performed. Using the photobioreactor model and parameters, the optimal input trajectories of the two nutrient feeds and light intensity were calculated for the

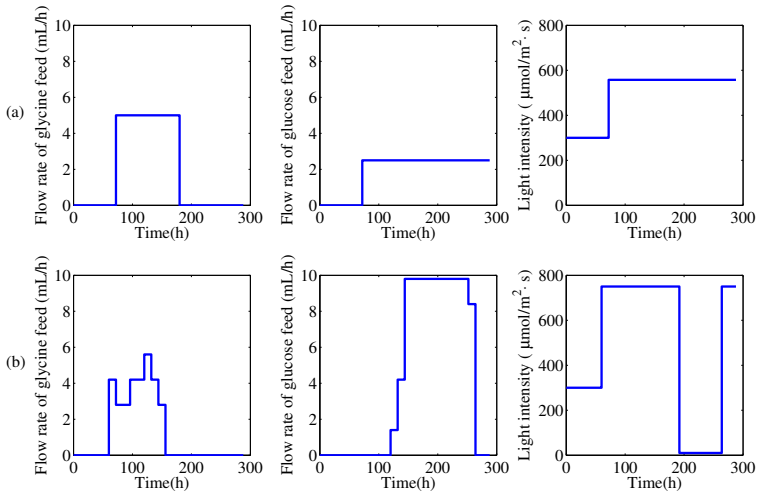

Figure 21: Designed input signals ((a) Designed inputs based on user experience; (b) Optimal inputs obtained by open-loop optimization)

maximization of the biomass and lipid concentration.

$$
\begin{aligned}
u^* &= \max_{u \in U} (X + 2L) \\
0 &\leq f_1^i \leq 10, \\
0 &\leq f_2^i \leq 10, \\
10 &\leq I \leq 750, \\
V_0 &+ \sum_{t_i}^{t_f} (f_1^i(t) + f_2^i(t) - f_0(t)) \leq V_{reactor}
\end{aligned}
\tag{5.10}
$$

The weight of lipid component in the objective function is twice larger than biomass to give more weight to the lipid component with considering sclae of biomass and lipid. To prevent the reactor overflowing by the input feeds, it was constrained that cultivation media

and input feeds do not exceed the reactor volume. The optimal input trajectories were calculated by solving optimization problem in Eq. (5.10), considering all the constraints. It was assumed that 3 input variables are manipulated every 12 h between 60 h and termination time, 288 h. Then, the number of optimization variables $(u_1, \ldots, u_f)$ was 57 within calculation time and the optimization problem was solved using the genetic algaorithm and pattern search tool available in Matlab. The calculated optimal input profiles are shown in Fig. 21, (b) and this input profiles are implemented during the cultivation of microalgae.

5.4.3 Model predictive control

Finally, for the purpose of control of the photobioreactor, model predictive control based on successive linearizations is implemented [59]. While microalgae were cultivated, there are many chances of occuring unknown metabolic reactions or phenomena which makes model mismatches to the real plant [58]. In such case, model predictive control can be used to track the reference trajectory. Model predictive control uses model to predict future behaviour of the system and optimize the input actions in order to give optimal action to reach a desired target [59]. In this study, maximized biomass and lipid trajectory obtained by applying optimal inputs calcultated from open-loop optimization method above were used as reference trajectory. Simulation studies firstly performed to determine user chosen parameter values; the prediction horizon (p), control horizon (m), weighting matrices in the objective function (G and W), and then model predictive control was performed experimently.

The objective function is the predicted deviation of the output from the target trajectory plus some penalty on the input movement size as in Eq. (5.11) [59].

$$\min_{\Delta u} \sum_{i=1}^{P} \begin{bmatrix} r(k+1|k)-y(k+1|k) \\ r(k+2|k)-y(k+2|k) \\ \vdots \\ r(k+p|k)-y(k+p|k) \end{bmatrix}^T \begin{bmatrix} G & & & \\ & G & & \\ & & \ddots & \\ & & & G \end{bmatrix} \begin{bmatrix} r(k+1|k)-y(k+1|k) \\ r(k+2|k)-y(k+2|k) \\ \vdots \\ r(k+p|k)-y(k+p|k) \end{bmatrix} + \sum_{l=0}^{m-1} \begin{bmatrix} \Delta u(k|k) \\ \Delta u(k+1|k) \\ \vdots \\ \Delta u(k+m-1|k) \end{bmatrix}^T \begin{bmatrix} W & & & \\ & W & & \\ & & \ddots & \\ & & & W \end{bmatrix} \begin{bmatrix} \Delta u(k|k) \\ \Delta u(k+1|k) \\ \vdots \\ \Delta u(k+m-1|k) \end{bmatrix} \tag{5.11}$$

In Eq. (5.11), $y(k+i|k)$ is the output $y(k+i)$ (biomass and lipid concentration) calculated from information available at time k, $u(k+l|k)$ is the inputs calculated from information available at time k. The set-point, $r(k+i)$, is the maximized biomass and lipid trajectory obtained from open-loop optimization.

The predicted output $y(k+i|k)$ is calculated by Eq. (5.12) and feed-

forward term such as known disturbance is neglected in this study.

$$\begin{bmatrix} y(k+1|k) \\ y(k+2|k) \\ \vdots \\ y(k+p|k) \end{bmatrix} = \underbrace{\begin{bmatrix} \widetilde{y}(k+1|k) \\ \widetilde{y}(k+2|k) \\ \vdots \\ \widetilde{y}(k+p|k) \end{bmatrix}}_{effect\ of\ past\ input} + \underbrace{\begin{bmatrix} S_1^d \\ S_2^d \\ \vdots \\ S_n^d \end{bmatrix}}_{feedforward\ term} \Delta d(k) + \underbrace{\begin{bmatrix} y_m(k)-\widetilde{y}(k|k) \\ y_m(k)-\widetilde{y}(k|k) \\ \vdots \\ y_m(k)-\widetilde{y}(k|k) \end{bmatrix}}_{feedback\ term} + \underbrace{\begin{bmatrix} S_1^u & 0 & \cdots & 0 \\ \vdots & \vdots & & \\ S_m^u & S_{m-1}^u & \cdots & S_1^u \\ \vdots & \vdots & & \vdots \\ S_p^u & S_{p-1}^u & \cdots & S_{p-m+1}^u \end{bmatrix}}_{dynamic\ matrix(S_u)} \underbrace{\begin{bmatrix} \Delta u(k|k) \\ \Delta u(k+1|k) \\ \vdots \\ \Delta u(k+m-1|k) \end{bmatrix}}_{future\ input\ moves} \tag{5.12}$$

Microalgal photobioreactor model can be expressed following nonlinear differential in Eq. (5.13).

$$\begin{aligned} \dot{z} &= f(z,u) \\ y &= h(z) \end{aligned} \tag{5.13}$$

where z is state vector, y is the measurement. By linearization of first order approximation of Eq. (5.13), the linearized model can be obtained and after discretization of the continuous linearized model, discrete time linear state-space form can be obtained as follows :

$$\begin{aligned} z_{k+1} &= Az_k + Bu_k \\ y_k &= Cz_k \end{aligned} \tag{5.14}$$

Then, dynamic matrix (S_u) can be calculated by the principle of superposition from the above equation at every sample time and can be expressed in Eq. (5.15).

$$S_u = \begin{bmatrix} CB & 0 & \cdots & 0 \\ C(AB+B) & CB & & \\ \vdots & \vdots & & \\ \sum_{i=0}^{m-1} CA^iB & \sum_{i=0}^{m-2} CA^iB & \cdots & CB \\ \vdots & \vdots & & \vdots \\ \sum_{i=0}^{p-1} CA^iB & \sum_{i=0}^{p-2} CA^iB & \cdots & \sum_{i=0}^{p-m} CA^iB \end{bmatrix} \tag{5.15}$$

Open loop prediction vector $\widetilde{y}(k+i|k)$ is computed by integrating the ODEs in Eq. (5.13) every sampling time with fixed input using Matlab ODE solver.

From Eq. (5.12), predicted output $y(k+i|k)$ can be obtained and by substitution of it to Eq. (5.11), optimization problem can be formulated. For the calculation of optimization problem, objective function in Eq. (5.11) is changed to the following form of quadratic program :

$$\begin{aligned} \min_{\Delta u} (\varepsilon^T(k)\overline{G}\varepsilon(k) - \underbrace{2\varepsilon^T(k)\overline{G}S^u}_{g^T}\Delta u(k) \\ +\Delta u^T(k)\underbrace{(S^{uT}\overline{G}S^u + \overline{W})}_{J}\Delta u(k) \end{aligned} \tag{5.16}$$

where J : hessian matrix, g : gradient vector, Δu : decision variable, $\varepsilon(k) = R(k+1|k) - Y(k+1|k) - S^d\Delta d(k) - Ip(y(k) - \widetilde{y}(k/k))$. The hessian J is a constant matrix while the gradient vector $g(k)$ must be updated at each time step. Additionally, the following input

and output (volume) constraints were also considered.

$$\begin{aligned} u_{min} \leq & u(k+l|k) \leq u_{max} \\ |\Delta u(k+l|k)| \leq & \Delta u_{max}, \quad l = 0, \ldots, m-1 \\ V_{min} \leq & V(k+j|k) \leq V_{max}, \quad j = 1, \ldots, p \end{aligned} \tag{5.17}$$

where u is the vector of inputs which is composed of [glycine feed, glucose feed, light intensity] and u_{min} and u_{max} are minimum and maximum value of inputs and selected as $[0, 0, 10]$ and $[10, 10, 750]$, respectively. Δu_{max} selected as $[5, 5, 500]$ and V_{min} and V_{max} are the minimum and maximum reactor volumes and selected as 1 L and 3L, respectively.

The computed control moves are impemented in receding horizon fashion; first, optimization problem is calculated at time k over the prediction horizon of p time steps. Then, only the first move Δu_k is implemented for the calculation of next output. In the next step, experimental data obtained from biomass sensor and lipid estimates were used as feedback for the complementation of the difference between output prediction and measured outputs. After that, the whole optimization procedures are repeated at the next sampling time.

5.5 Results and Discussion

5.5.1 Manual operation based on algal growth characteristic

C. prothothecoides were cultivated with the inputs shown in Fig. 21, (a) to improve the productivity of biomass and lipid based on the user experiences. Experiment and simulation were performed

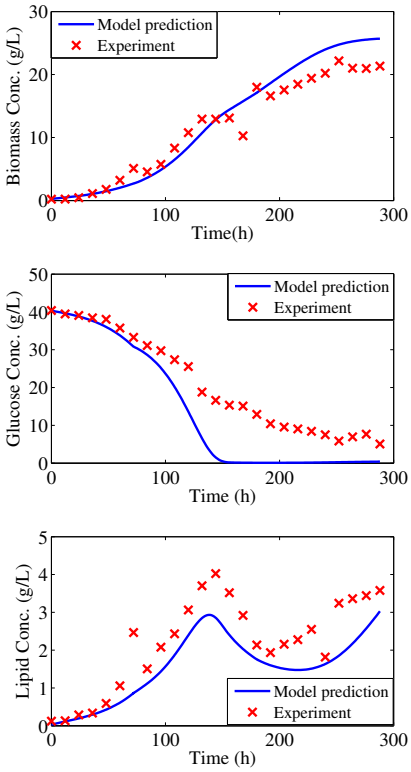

Figure 22: Simulation and experimental results of optimization based on user experience

and results were shown in Fig. 22. Although there are some discrepancies, model prediction values show good agreement with the experimental results especially in biomass and lipid concentrations. For the biomass concentration, 21.33 g/L of biomass concentration was obtained and this value is greatly improved one compared with previous study by Yoo et al. (2014), whose experiments were designed for the parameter estimation. However, for the lipid concentration, it

did not show a satisfactory level of productivity with only 10-20 % of lipid contents in algal cells. In spite of low lipid productivities, lipid concentration increases at the termination perioid of the cultivation with the beginning of color changes of $protothecoides$ from green to yellow. $Protothecoides$ show yellow color in lipid rich conditions. Therefore, it is expected that lipid concentration can be increased more if cultivation time was longer than 288 h. Overall, the initial intend to grow microaglae first, and then to accumulate lipid is partly mathced with the needs of manipulation to accumulate more lipids.

5.5.2 Open-loop optimization

Opne-loop optimization was performed using the obtained inputs in Fig. 21, (b) and the results of experiment and simulation run were represented in Fig. 23. The simulation results of the biomass and lipid concentration were significantly increased and almost 25 g/L and 16 g/L were obtained, respectively. The high concentration of biomass and lipid in simulation is natural because the inputs are optimal trajectories for maximizing the biomass and lipid concentration. The problem is whether it can be reproduced from the experiments. However, the results of experimental data showed large differences with simulation results especially when cultivation time passed 150 h. Such a large difference seems to be strange even though considering model-plant mismatches. It was thought that the growth of microalgae was paused for some time after 150 h. In fact, this period matches with the time that large amount of glucose feeds into the reactor as shown in Fig. 21, (b). During this period, 9.8 ml/h of glucose feed was introduced from 144 h to 252 h and in this period, glucose

concentration was almost not consumed from the experimental data. However, although 9.8 ml/h of glucose feed was introduced from 144 h to 252 h, the glucose concentration was decreased again from 216 h, which means the growth or activation of microalgae reactivated about that time. Therefore, it was thought that the lag phase occurs to adapt themselves to abruptly changed growth conditions which was caused by large amount of input feeds. From those results, when mi-

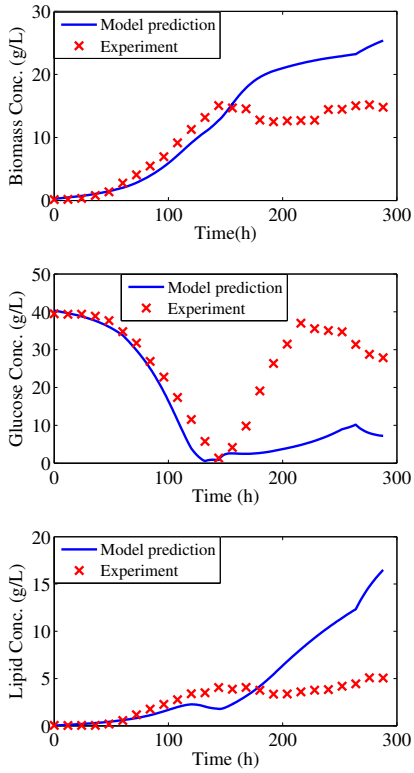

Figure 23: Simulation and experimental results using open-loop optimization method

croalgae were cultivated for the control or optimization purposes, it is important to consider these phenomena into the model, which is a very difficult task, or to constrain the feed conditions not to happen lag phase. This is very important factor which can make model-plant mismatches, but have never considered in other simulation studies for optimization of algal production.

5.5.3 Model predictive control

5.5.3.1 Simulation results

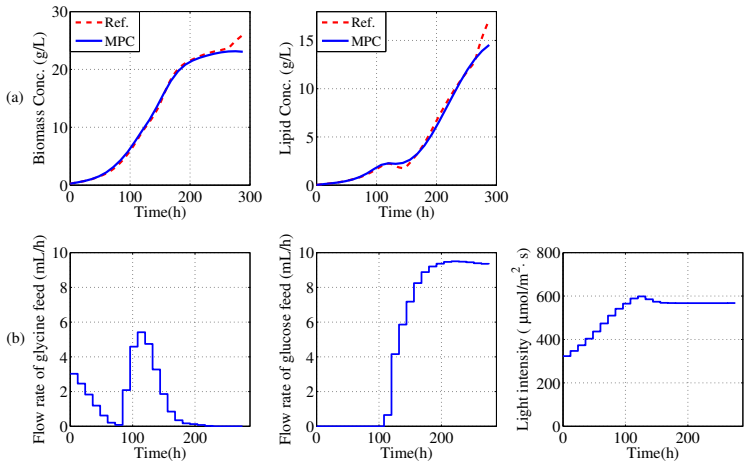

Figure 24: Simulation results of model predictive control ((a) Reference trajecctory tracking of biomass and lipid concentration; (b) Optained inputs by MPC calculation)

Simulation studies of MPC were performed to determine user chosen parameters with tracking the reference trajectory well. Initially, prediction horizon (p) and control horizon (m) were determined considering simulation time. Because the termination time was fixed

as 288 h, simulation times are shrinking as experiment progressed. Therefore, predition horizon was determined as from current time to termination time and control horizon was determined as the half value of prediction horizon as in Eq. (5.18).

$$\begin{aligned} t_r &= 288 - t_c \\ p &= t_r/t_s \\ m &= round(p/2) \;\; (t_r > 12) \\ m &= 1 \;\; (t_r = 12) \end{aligned} \tag{5.18}$$

where t_r is the residual time, t_c is the current time, t_s is the sampling time, and round means nearest integers. For the weighting matrices, G and W were selected as $G = \mathrm{diag}([2, 2])$ and $W = \mathrm{diag}([5, 5, 0.005])$, respectively.

The simulation results of this condition are shown in Fig. 24. MPC can track the reference trajectory satisfactorily.

5.5.3.2 Experimental results

$C. protothecoides$ were cultivated in a photobioreactor using the inputs obtained from MPC calculation. Every sampling time, biomass sensor data and glucose HPLC data analyzed instantly within one hour and these data were applied in estimation of lipid concentration using UKF. After that, biomass sensor data and estimated lipid data were used for tracking the reference trajectory using MPC. After calculation of MPC, the obtained inputs were applied in the photobioreactor and these steps are repeated in the next sampling time. Then, there happens one hour of delay from sampling to applying

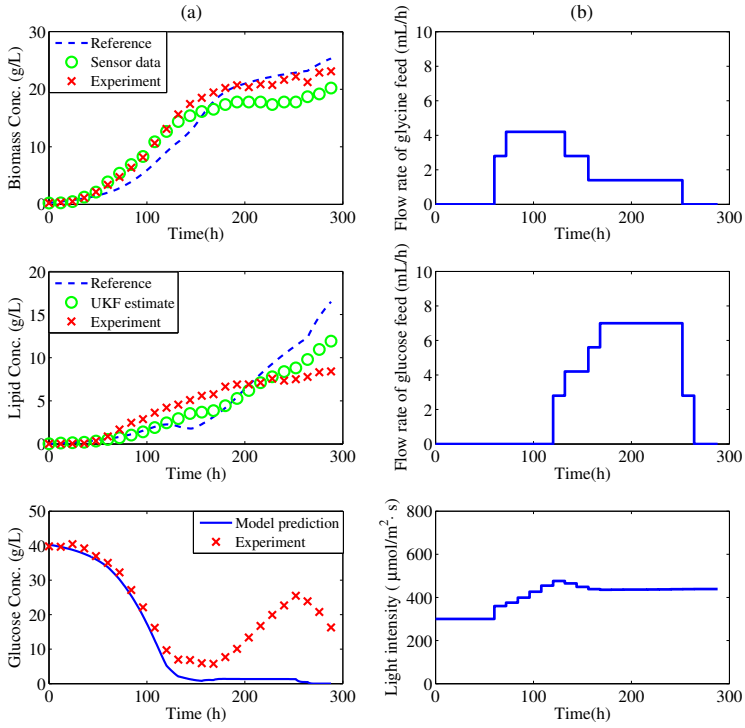

Figure 25: Experimental results and obtained inputs using MPC ((a) Experimental results of MPC with biomass sensor data and lipid estimate; (b) Optained inputs by MPC calculation)

new inputs to the photobioreactor. However, one hour of delay was neglected and it was assumed that real-time output data were obtained when UKF and MPC were performed. This is because the changes of microalgae in photobioreactor during one hour are very small and are in the range of experimental errors. Although, not used in the calculation of MPC, the biomass and lipid concentration also anlyzed experimentaly for the comparison purposes.

The results of MPC implementation and calculated inputs are

shown in Fig. 25. Compared with previous two method, high concentration of biomass and lipid with 23.13 g/L and 8.41 g/L was obtained, respectively. Especially, 8.41 g/L of lipid concentration was very improved one compared with previous methods and $C. protothecoides$ showed yellow color during whole cultivation time. Futhermore, experimental data were more close to the reference trajectory than open-loop optimization method. However, there are also some delays in growth of microalgae between 180 h and 228 h with small amount of glucose consumption, which makes large difference in glucose data with model prediction results.

The main factor for productivity improvement of MPC comes from the data feedback in the MPC calculation. The most ideal results of experimental data with open-loop optimization and MPC must have same with simulation results of open-loop optimization. This is because reference trajectories of MPC are obtained from open-loop optimization results. However, there are many uncertainties when microalge grow and it may cause some mismatch with simulation results when the inputs calculated before cultivation were used. In such case, data obtained every 12 h can be used as feedback for the complementation of the difference between output predictions and measured outputs.

The results of cultivation with three different method were compared in Fig. 26. When MPC was used, the maximum biomass and lipid concentration were obtained.

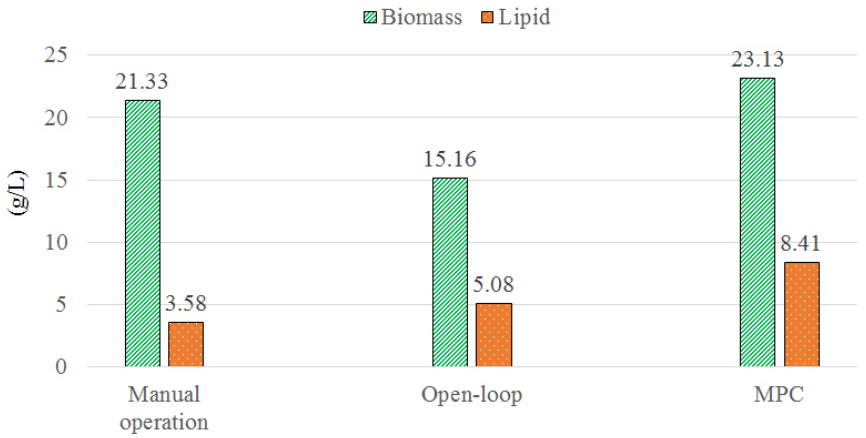

Figure 26: Comparison of product concentration with different optimization methods

5.6 Conclusions

For the improvement of biomass and lipid productivity, optimization of microalgal photobioreactor system was performed. Optimal input trajectory was obtained with open-loop optimization and was used as a reference trajectory for MPC. The importance of this study is that near real-time optimization with existence of one hour of delay was applied not only simulation but also experimentally. The results also show significant increase in biomass and lipid productivity when inputs from MPC calculation was applied.

Chapter 6

Concluding Remarks

This thesis has presented the near real-time optimization procedures for productivity improvement of microalgal photobioreactor system under mixotrophic cultivation with experimental validation. For this purpose, $Chlorella\ prototheco\acute{i}des$ were cultivated in the photobioreactor system which can manipulates operating conditions such as nutrient feed flow rates and light intensity. In order to explain the photobioreactor system, photobioreactor model was deveoped at first based on Droop model to predict the productivity of biomass and lipid concentration. A novel model based on the experimental observations of lipid depletion was proposed with time-varying yield coefficients which reduce the number of parameters. The results suggest that the dynamics of lipid are relatively fast and it is important to cultivate microalgae within the conditions of lipid increase. With its capability of representing various operating scenarios, the proposed model will be useful in a model based control strategy to improve the productivity of biomass and lipid.

After that, estimation of lipid concentration in microalgal photobioreactor system was studied. It was found that EKF was not suitable for estimating lipid concentration in most cases while UKF and PF showed satisfactory performances. Finally, experimental validation

was performed that suggested time-varying system noise covariance with a biomass sensor and infrequent glucose lab data can improve the estimation performance significantly. However, there are some limitations in applying this method that model has to be accurate for estimating unmeasured variables. If the model is not accurate, parameter update by estimation of key parameters is one way to enhance the robustness of the estimator.

Finally, for the improvement of biomass and lipid productivity, optimization of microalgal photobioreactor system was performed. Optimal input trajectory was obtained with open-loop optimization and it was used as a reference trajectory for MPC. The importance of this study is that near real-time optimization method was applied not only simulation but also experimentally. The results also show significant increase in biomass and lipid productivity when inputs from MPC calculation was applied. However, it was observed that a lag phase was occurred when large amount of inputs were introduced to the photobioreactor, which must be solved or constrained for improvement of productivity.

Bibliography

[1] C. Yusuf, Biodiesel from microalgae, Biotechnology Advances 25 (3) (2007) 294–306.

[2] X. Miao, Q. Wu, Biodiesel production from heterotrophic microalgal oil, Bioresource Technology 97 (6) (2006) 841–846.

[3] T. Minowa, S.-y. Yokoyama, M. Kishimoto, T. Okakura, Oil production from algal cells of dunaliella tertiolecta by direct thermochemical liquefaction, Fuel 74 (12) (1995) 1735–1738.

[4] M. Xiao, H.-J. Shin, Q. Dong, Advances in cultivation and processing techniques for microalgal biodiesel: A review, Korean Journal of Chemical Engineering 30 (12) (2013) 2119–2126.

[5] H.-S. Song, F. DeVilbiss, D. Ramkrishna, Modeling metabolic systems: the need for dynamics, Current Opinion in Chemical Engineering 2 (4) (2013) 373–382.

[6] X. Li, H. Xu, Q. Wu, Large-scale biodiesel production from microalga chlorella protothecoides through heterotrophic cultivation in bioreactors, Biotechnology and Bioengineering 98 (4) (2007) 764–771.

[7] F. Chen, High cell density culture of microalgae in heterotrophic growth, Trends in Biotechnology 14 (11) (1996) 421–426.

[8] Y. Liang, N. Sarkany, Y. Cui, Biomass and lipid productivities of chlorella vulgaris under autotrophic, heterotrophic and mixotrophic growth conditions, Biotechnology Letters 31 (7) (2009) 1043–1049.

[9] J. Pruvost, G. V. Vooren, G. Cogne, J. Legrand, Investigation of biomass and lipids production with neochloris oleoabundans in photobioreactor, Bioresource Technology 100 (23) (2009) 5988–5995.

[10] F. Mairet, O. Bernard, P. Masci, T. Lacour, A. Sciandra, Modelling neutral lipid production by the microalga isochrysis aff. galbana under nitrogen limitation, Bioresource Technology 102 (1) (2011) 142–149.

[11] S. J. Yoo, J. H. Kim, J. M. Lee, Dynamic modelling of mixotrophic microalgal photobioreactor systems with time-varying yield coefficient for the lipid consumption, Bioresource Technology 162 (0) (2014) 228–235.

[12] A. J. de Assis, R. M. Filho, Soft sensors development for on-line bioreactor state estimation, Computers and Chemical Engineering 24 (2–7) (2000) 1099–1103.

[13] L. Dewasme, G. Goffaux, A.-L. Hantson, A. V. Wouwer, Experimental validation of an extended kalman filter estimating acetate concentration in e. coli cultures, Journal of Process Control 23 (2) (2013) 148–157.

[14] M. Morari, G. Stephanopoulos, Optimal selection of secondary measurements within the framework of state estimation in the presence of persistent unknown disturbances, AIChE Journal 26 (2) (1980) 247–260.

[15] J. Henderson, R. D. Ricker, B. A. Bidlingmeyer, C. Woodward, Rapid, accurate, sensitive, and reproducible hplc analysis of amino acids, Amino acid analysis using Zorbax Eclipse-AAA columns and the Agilent 1100 (2000) 1–10.

[16] W. Chen, C. Zhang, L. Song, M. Sommerfeld, Q. Hu, A high throughput nile red method for quantitative measurement of neutral lipids in microalgae, Journal of Microbiological Methods 77 (1) (2009) 41–47.

[17] R. Halim, B. Gladman, M. K. Danquah, P. A. Webley, Oil extraction from microalgae for biodiesel production, Bioresource Technology 102 (1) (2011) 178–185.

[18] R. Halim, M. K. Danquah, P. A. Webley, Extraction of oil from microalgae for biodiesel production: A review, Biotechnology Advances 30 (3) (2012) 709–732.

[19] M. Droop, Vitamin b12 and marine ecology. iv. the kinetics of uptake, growth and inhibition in monochrysis lutheri, Journal of the Marine Biological Association of the United Kingdom 48 (3) (1968) 689–733.

[20] J. Yang, E. Rasa, P. Tantayotai, K. M. Scow, H. Yuan, K. R. Hristova, Mathematical model of chlorella minutissima utex2341 growth and lipid production under photoheterotrophic fermentation conditions, Bioresource Technology 102 (3) (2011) 3077–3082.

[21] K. Surisetty, H. D. l. Hoz Siegler, W. C. McCaffrey, A. Ben-Zvi, Model re-parameterization and output prediction for a bioreactor system, Chemical Engineering Science 65 (16) (2010) 4535–4547.

[22] H. D. la Hoz Siegler, A. Ben-Zvi, R. Burrell, W. McCaffrey, The dynamics of heterotrophic algal cultures, Bioresource Technology 102 (10) (2011) 5764–5774.

[23] J. Lobry, J. Flandrois, G. Carret, A. Pave, Monod's bacterial growth model revisited, Bulletin of Mathematical Biology 54 (1) (1992) 117–122.

[24] J. Monon, The growth of bacterial cultures, Annual Review of Microbiology 3 (1949) 371–394.

[25] H.-H. Wang, M. Krstic, G. Bastin, Optimizing bioreactors by extremum seeking, International Journal of Adaptive Control and Signal Processing 13 (8) (1999) 651–669.

[26] J. Caperon, J. Meyer, Nitrogen-limited growth of marine phytoplankton—ii. uptake kinetics and their role in nutrient limited growth of phytoplankton, Deep Sea Research and Oceanographic Abstracts 19 (9) (1972) 619–632.

[27] P. Tett, M. Droop, Cell quota models and planktonic primary production, in: Handbook of laboratory model systems for microbial ecosystems 2 (1988) 177–233.

[28] P. Eilers, J. Peeters, Dynamic behaviour of a model for photosynthesis and photoinhibition, Ecological Modelling 69 (1–2) (1993) 113–133.

[29] J. T. Lehman, D. B. Botkin, G. E. Likens, The assumptions and rationales of a computer model of phytoplankton population dynamics, Limnol. Oceanogr 20 (3) (1975) 343–364.

[30] Biology of Plants,(7th ed.), New York: WH Freeman and Company.

[31] K. Z. Yao, B. M. Shaw, B. Kou, K. B. McAuley, D. W. Bacon, Modeling ethylene/butene copolymerization with multisite catalysts: Parameter estimability and experimental design, Polymer Reaction Engineering 11 (3) (2003) 563–588.

[32] J. Stigter, K. Keesman, Optimal parametric sensitivity control of a fed-batch reactor, Automatica 40 (8) (2004) 1459–1464.

[33] Y. Bard, Nonlinear parameter estimation, Vol. 1209, Academic Press New York, 1974.

[34] C. Sorokin, R. W. Krauss, The effects of light intensity on the growth rates of green algae., Plant physiology 33 (2) (1958) 109–113.

[35] D. P. Maxwell, S. Falk, N. P. Huner, Photosystem ii excitation pressure and development of resistance to photoinhibition (i. light-harvesting complex ii abundance and zeaxanthin content in chlorella vulgaris), Plant Physiology 107 (3) (1995) 687–694.

[36] M. E. Martínez, F. Camacho, J. Jiménez, J. Espinola, Influence of light intensity on the kinetic and yield parameters of chlorella pyrenoidosa mixotrophic growth, Process biochemistry 32 (2) (1997) 93–98.

[37] T. Roach, A. Sedoud, A. Krieger-Liszkay, Acetate in mixotrophic growth medium affects photosystem ii in chlamydomonas reinhardtii

and protects against photoinhibition, Biochimica et Biophysica Acta (BBA) - Bioenergetics 1827 (10) (2013) 1183–1190.

[38] J. Albiol, J. Robuste, C. Casas, M. Poch, Biomass estimation in plant cell cultures using an extended kalman filter, Biotechnology Progress 9 (2) (1993) 174–178.

[39] C. Komives, R. S. Parker, Bioreactor state estimation and control, Current Opinion in Biotechnology 14 (5) (2003) 468–474.

[40] D. D. Y. Ryu, S. O. Lee, R. J. Romani, Determination of growth rate for plant cell cultures: Comparative studies, Biotechnology and Bioengineering 35 (3) (1990) 305–311.

[41] W. W. Su, J. Li, N.-S. Xu, State and parameter estimation of microalgal photobioreactor cultures based on local irradiance measurement, Journal of Biotechnology 105 (1–2) (2003) 165–178.

[42] S.-K. Oh, S. J. Yoo, D. H. Jeong, J. M. Lee, Real-time estimation of glucose concentration in algae cultivation system using raman spectroscopy, Bioresource Technology 142 (0) (2013) 131–137.

[43] M. Arulampalam, S. Maskell, N. Gordon, T. Clapp, A tutorial on particle filters for online nonlinear/non-gaussian bayesian tracking, Signal Processing, IEEE Transactions on 50 (2) (2002) 174–188.

[44] R. Kandepu, B. Foss, L. Imsland, Applying the unscented kalman filter for nonlinear state estimation, Journal of Process Control 18 (7–8) (2008) 753–768.

[45] X. Shao, B. Huang, J. M. Lee, Constrained bayesian state estimation – a comparative study and a new particle filter based approach, Journal of Process Control 20 (2) (2010) 143–157.

[46] A. Romanenko, J. A. Castro, The unscented filter as an alternative to the ekf for nonlinear state estimation: a simulation case study, Computers and Chemical Engineering 28 (3) (2004) 347–355.

[47] D. Simon, Optimal state estimation: Kalman, H infinity, and nonlinear approaches, John Wiley & Sons, 2006.

[48] R. Radakovits, R. E. Jinkerson, A. Darzins, M. C. Posewitz, Genetic engineering of algae for enhanced biofuel production, Eukaryotic cell 9 (4) (2010) 486–501.

[49] T. G. Dunahay, E. E. Jarvis, S. S. Dais, P. G. Roessler, Manipulation of microalgal lipid production using genetic engineering, in: Seventeenth Symposium on Biotechnology for Fuels and Chemicals, 1996, pp. 223–231.

[50] S. Tebbani, F. Lopes, G. B. Celis, Nonlinear control of continuous cultures of porphyridium purpureum in a photobioreactor, Chemical Engineering Science 123 (0) (2015) 207–219.

[51] S. Ramaswamy, T. Cutright, H. Qammar, Control of a continuous bioreactor using model predictive control, Process Biochemistry 40 (8) (2005) 2763 – 2770.

[52] Z. Li, H. Yuan, J. Yang, B. Li, Optimization of the biomass production of oil algae chlorella minutissima utex2341, Bioresource Technology 102 (19) (2011) 9128–9134.

[53] D. Hu, H. Liu, C. Yang, E. Hu, The design and optimization for light-algae bioreactor controller based on artificial neural network-model predictive control, Acta Astronautica 63 (7–10) (2008) 1067–1075.

[54] J. Abdollahi, S. Dubljevic, Lipid production optimization and optimal control of heterotrophic microalgae fed-batch bioreactor, Chemical Engineering Science 84 (0) (2012) 619–627.

[55] M. Farza, H. Hammouri, S. Othman, K. Busawon, Nonlinear observers for parameter estimation in bioprocesses, Chemical Engineering Science 52 (23) (1997) 4251–4267.

[56] L. Mailleret, O. Bernard, J.-P. Steyer, Nonlinear adaptive control for bioreactors with unknown kinetics, Automatica 40 (8) (2004) 1379–1385.

[57] H. D. la Hoz Siegler, W. McCaffrey, R. Burrell, A. Ben-Zvi, Optimization of microalgal productivity using an adaptive, non-linear model based strategy, Bioresource Technology 104 (0) (2012) 537–546.

[58] S. J. Yoo, D. H. Jung, J. H. Kim, J. M. Lee, A comparative study of soft sensor design for lipid estimation of microalgal photobioreactor system with experimental validation, Bioresource Technology 179 (0) (2015) 275–283.

[59] J. H. Lee, M. Morari, C. E. Garcia, Model predictive control, Preprint, 2003.

초 록

본 논문은 혼합영양 하에서 미세조류 배양 광생물반응기의 생산성 향상을 위한 근실시간 최적화 방법에 대하여 다루고 있다. 미세조류는 지질 생산성이 뛰어난 특성을 가지고 있어서 바이오 연료 생산을 위한 유망한 원료로서 많이 연구되어 왔지만 높은 생산 비용에 의하여 대규모의 미세조류 생산에 의한 상업화에는 제약이 있어왔다. 따라서, 생산성 향상에 의한 가격 경쟁력 향상이 필요하며, 본 논문에서는 영양분(탄소성분, 질소성분)과 광량 등의 조업 변수를 최적으로 조절함으로써 배양공정을 최적화하고자 하였다.

이러한 바이오 공정의 스케일업, 최적화 및 제어를 위해 반응기 내 미세조류 성장 및 지질의 축적을 설명할 수 있는 동적 모델의 개발이 필요하다. 하지만, 이러한 모델에 기반한 제어 기법을 미세조류 배양 시스템에 적용하는데에는 어려움이 있는데, 먼저, 미세조류 성장은 복잡한 생확학 반응들로 이루어져 있어서 모델링 하기가 쉽지 않으며, 복잡한 대사과정 특성상 배양 과정에서 많은 불확실성을 가지고 있다. 다음으로, 실시간 최적화를 위해서는 주요 변수들의 정보가 필요하나, 지질의 경우 분석이 어렵고 시간이 오래걸리는 특성이 있어서 온라인 측정 정보를 얻기가 쉽지가 않다. 이러한 점에 착안하여, 본 연구에서는 미세조류 배양 시스템의 모델링, 상대적으로 얻기 쉬운 바이오매스와 글루코즈 데이터를 이용한 지질의 농도 추정, 그리고 최종적으로 모델과 추정 기법을 이용한 최적화에 초점을 두었다.

먼저, 드룹모델에 기반하여 모델을 개발하였으며, 개발한 모델의 파라미터 추정을 위하여 더 많은 정보를 줄 수 있는 입력량을 구하기 위하여 최적 입력 설계를 수행하였다. 최적 입력 설계

를 통해 얻은 입력량을 실제 실험에 적용하여 실험을 진행하였으며, 그 결과 수율 계수 (yield coefficient)를 새롭게 정의함으로써 셀 내부의 지질과 질소에 관한 소모율을 추가적인 파라미터 없이 나타낼 수 있었다. 개발 된 모델이 다른 조건의 실험에서도 적용가능한지 실증 실험을 진행을 하였고, 모델이 실험결과를 잘 설명함을 확인 할 수 있었다.

다음으로, 상대적으로 측정이 쉬운 바이오매스와 글루코즈 데이터를 이용한 지질의 농도 추정을 수행하였다. 확정 칼만 필터 (extended Kalman filter), 언센티드 칼만 필터 (unscented Kalman filter), 그리고 파티클 필터 (particle filter) 의 광생물 반응기에 적용가능성을 확인하기 위하여 다양한 케이스에 대하여 비교 연구를 수행하였으며, 지질 추정에 적합한 센서 종류를 결정하기 위하여 여러가지 센서 종류에 대하여 비교 연구를 수행하였다.

최종적으로, 바이오매스와 지질의 농도를 최대화하기 위하여 여러가지 최적화 방법에 의하여 시뮬레이션 및 실험을 수행하였다. 미세조류 성장 특성을 반영한 최적화, 모델을 이용한 개루프 (Open-loop) 최적화, 모델 예측 제어(Model predictive control)를 수행 하였으며, 모델 예측 제어에 이용하기 위한 지질의 농도 정보는 언센티드 칼만 필터를 수행하여 얻어진 정보를 이용하였고, 모델 예측 제어에서 따르고자 하는 최대 바이오매스와 지질의 농도 궤적은 개루프 최적화에서 얻어진 바이오매스와 지질의 농도 궤적을 이용하였다. 그 결과, 모델 예측 제어를 수행한 경우 높은 바이오매스와 지질의 생산성을 얻을 수 있었다.

최적화를 위한 실험 진행 과정에서, 영양분과 같은 조절 변수를 넣어주는 과정중에 미세조류의 성장이 일시적으로 멈추는 것과 같은 현상을 보였는데, 유도기 (lag phase)가 발생한 것으로 여겨진다. 이는 모델과 플랜트간의 차이를 발생할 수 있는 중요한 현상이며, 따라서 최적화를 수행함에 있어서 유도기가 발생

하지 않도록 영양분의 주입량에 제약을 주는 등의 해결이 필요하다.

주요어 : 미세조류, 드룹모델, 최적 입력 설계, 파라미터 추정, 센서, 모델예측제어, 유도기
학번 : 2010-31013